University of Montana
ScholarWorks at University of Montana

Graduate Student Theses, Dissertations, & Professional Papers

Graduate School

2022

CAUSES AND CONSQUENCES OF FIRE IN FOREST ECOSYSTEMS OF THE SELWAY-BITTERROOT WILDERNESS

Melissa Jaffe

Follow this and additional works at: https://scholarworks.umt.edu/etd

 Part of the Natural Resources and Conservation Commons, and the Natural Resources Management and Policy Commons

Let us know how access to this document benefits you.

Recommended Citation
Jaffe, Melissa, "CAUSES AND CONSQUENCES OF FIRE IN FOREST ECOSYSTEMS OF THE SELWAY-BITTERROOT WILDERNESS" (2022). *Graduate Student Theses, Dissertations, & Professional Papers*. 11961.
https://scholarworks.umt.edu/etd/11961

This Thesis is brought to you for free and open access by the Graduate School at ScholarWorks at University of Montana. It has been accepted for inclusion in Graduate Student Theses, Dissertations, & Professional Papers by an authorized administrator of ScholarWorks at University of Montana. For more information, please contact scholarworks@mso.umt.edu.

CAUSES AND CONSQUENCES OF FIRE IN FOREST ECOSYSTEMS OF THE SELWAY-BITTERROOT WILDERNESS

By

MELISSA ROSE JAFFE

Ecosystem Management and Forestry B.S., University of California, Berkeley, CA, 2020

Environmental Science B.S., University of California, Berkeley, CA, 2020

Thesis

presented in partial fulfillment of the requirements

for the degree of

Master of Science

in Forestry

The University of Montana

Missoula, MT

Official Graduation Date (May 2022)

Approved by:

Ashby Kinch, Dean of The Graduate School

Andrew J. Larson, Chair

W.A. Franke College of Forestry and Conservation

Carl Seielstad

W.A. Franke College of Forestry and Conservation

Phillip Higuera

W.A. Franke College of Forestry and Conservation

Sean A. Parks

Aldo Leopold Wilderness Research Institute

Table of Contents

Chapter 1: Biophysical and geographic predictors of fire occurrence 1985-2020

Abstract

Understanding where and when wildfires occur on the landscape and their drivers helps us to better understand the patterns and processes of the disturbance regime. Forested ecosystems in the northern Rocky Mountains, and specifically the Selway-Bitterroot Wilderness (SBW), are excellent system in which to study modern active fire regimes because of the long time period of managed wildfire. Here, I investigate if there are intrinsic landscape differences between areas that have not burned, burned once, or burned twice or more from 1985 to 2020. I ask what topographic, climatic, biotic, and geographic factors impact how frequently fire occurs across the landscape. High mean (30-year average) climatic water deficit (CWD) is common in areas of multiple fires, and high annual CWD is associated with longer time between reburns, providing evidence for a climate-driven fire regime. The occurrence of reburns between 1985 and 2020 increased with increasing distance from the wilderness boundary, suggesting a potential spatial suppression bias in the wilderness fire regime. Upper slope topographic position index values were associated with more frequent fires and more areas with multiple fires. This is potentially indicative more lightning ignitions or more flammable (arid) fuels at higher slope positions. Fire resistance score (a metric quantifying tree community fire resistance based on individual species traits) had a bimodal distribution where low and high values were associated with shorter time between fires, and there was a longer time between fires for mid-range values of fire resistance score. Beyond distances of about nine kilometers from the wilderness boundary climatic and topographic variables had stronger influence on fire frequency, suggesting hierarchal control of fire management decisions on other fire regime drivers in the SBW.

Introduction

Disturbance and resilience are integral to each other. A resilient ecosystem not only withstands disturbance but requires it within a certain interval, severity, and size distributions to maintain structural and functional capabilities (Holling 1973, Hessburg et al. 2019). Understanding where and when disturbances occur on the landscape, and their drivers, helps us to understand the drivers of the disturbance regime and the mechanisms that underpin ecosystem resilience. Where fires occur on the landscape is caused by where ignitions occur (Barnett et al. 2016) and fire spread, which is in turn impacted by climate, topography, vegetation, and human influence.

Fire regimes are altered by human actions through the impact of fire suppression, exclusion and ignitions, climate change, anthropogenic ignitions, vegetation management, and land-use change (Steel et al. 2015, Higuera et al. 2015, Balch et al. 2017). It is important to understand both how fire regimes have functioned and how they will function in the face of these changes. Large wilderness areas are ideal places to study the patterns and processes of fire because of the reduction of potential confounding effects from human actions and less fire suppression in recent decades (Berkey et al. 2021b).

One of the key uses of Congressionally designated wilderness areas in the United States is scientific research—areas to be used as natural laboratories. This has allowed for fire to be studied as an ecological process (Collins et al. 2009, Boisramé et al. 2017, Kreider et al. 2022). The northern US Rocky Mountains, and specifically the Selway-Bitterroot Wilderness (SBW), are an excellent place to study the causes and consequences of fire because of the long period of managed wildfire (Habeck and Mutch 1973, Arno 1976, Parks et al. 2015a, Larson 2016). I use the SBW to study the modern (1985-2020) landscape fire regime and associated drivers. I investigate if are there intrinsic landscape differences between areas that have not burned, burned

once, or burned twice or more from 1985 to 2020. I also investigate if topographic, climatic, biological, and geographic factors impact the interval between recurring fires in a location.

Methods

Study Area

This research was conducted in the Selway-Bitterroot Wilderness (SBW), which is located the northern US Rocky Mountains, spanning the borders of Idaho and Montana, USA. It is the third largest congressionally designated wilderness in the contiguous United States at 5471 km^2. Its elevational range is 531 m to 3,096 m and has a mean annual precipitation of 1221 mm and mean annual temperature of 3.5°C (Parks et al. 2015a). Low and middle elevation forests in the SBW are composed of ponderosa pine (*Pinus ponderosa*) and Douglas-fir (*Pseudotsuga menziesii*) on warm and dry sites, with variable mixtures of western redcedar (*Thuja plicata*), grand fir (*Abies grandis*), western white pine (*Pinus monticola*), western larch (*Larix occidentalis*), and Engelmann spruce (*Picea engelmannii*) on mesic sites and at middle elevations. The higher elevation subalpine forests, which make up 70% of the SBW, are composed of subalpine fir (*Abies lasiocarpa*), lodgepole pine (*Pinus contorta*), whitebark pine (*Pinus albicaulis*), and subalpine larch (*Larix lyallii*) (Finklin 1983, Rollins et al. 2000, Berkey et al. 2021).

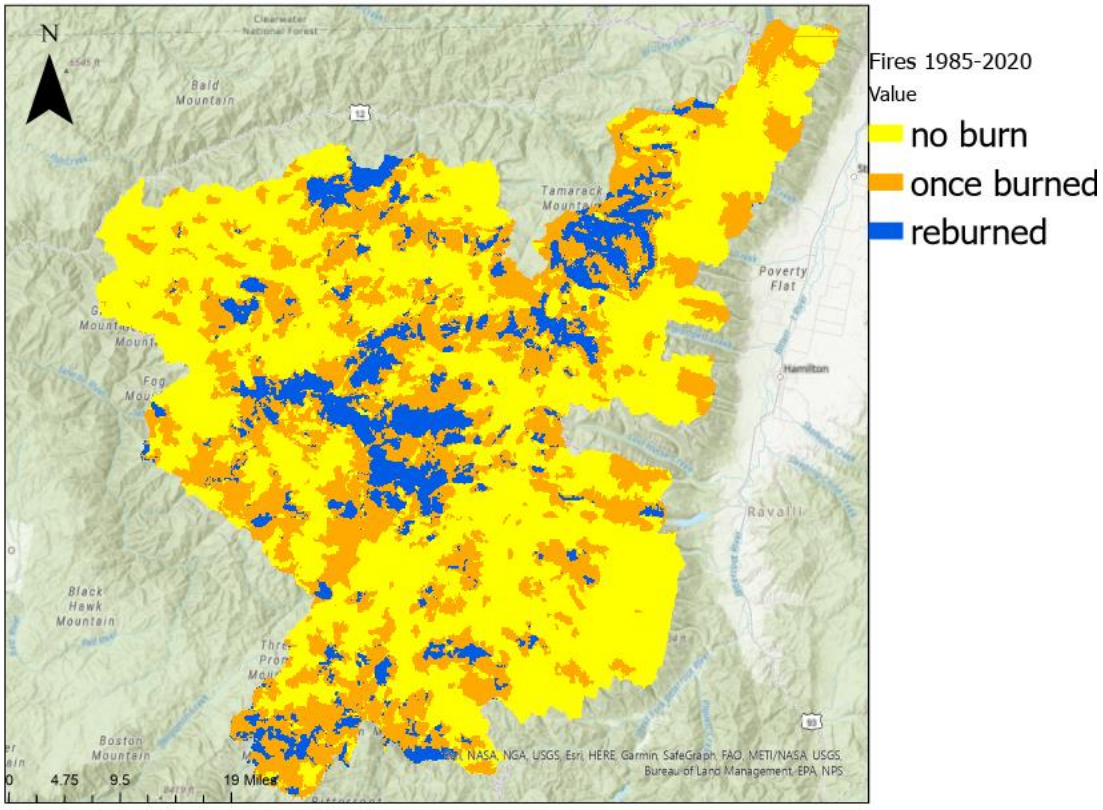

Figure 1. Selway-Bitterroot Wilderness differentiated by burn history from 1985 to 2020. "No burn" has not burned from 1985 to 2020, "once burned" has burned once and "reburned" has burned $\geq$ 2 times during the study period.

1985-2020 Burn History

Fire perimeters were identified across all of the SBW from 1985-2015 using the fire atlas of (Parks et al. 2015b), extended through the 2020 fire season (Appendix A). Unburnable areas, such as water, rock, and perennial snow, were masked out using LANDFIRE Existing Vegetation Type dataset (LANDFIRE 2016). Annual fire perimeters were converted to rasters at a 30-meter resolution and layered to determine how many times an area had burned. Fire interval is the time (in years) between the first and second fire in a reburn sequence. I calculated fire

interval for all fires greater than 20 ha from 1985-2020. The final dataset was 0.1% sample of these fires creating 911 independent observations of 900 m^2 pixels that were reburned.

Explanatory variables

I used topographic position index (TPI) at 30-meter resolution to characterize landform. TPI is a relative elevation metric, measuring the topographic position from a central point to determine the difference between the elevation at the focal point and the mean elevation within a predetermined neighborhood (Wilson and Gallant 2000). I used a 1000 m neighborhood to calculate TPI (Weiss 2001). TPI with a value of zero is the mid-point of the slope; if TPI is greater than zero then it is above mid-slope and if TPI is negative then it is below mid-slope.

To quantify average climate conditions, I used the average climate water deficit (CWD) over the 30-year period of 1981-2010. CWD is potential evapotranspiration minus actual evapotranspiration, representing the balance of water and energy inputs and outputs of a system (Stephenson 1998). High CWD values are indicative of high unmet evapotranspiration demand, where available water is not sufficient resulting in periods of drought stress, while low CWD is indicative of low unmet evapotranspiration demands—sufficient water relative to the prevailing energy environment. This was estimated using a Thorthwaite-type monthly water balance model (Kreider, personal correspondence) using temperature and precipitation data from PRISM gridded datasets to create 90-meter resolution data (PRISM 2018). I then interpolated this data to a 30-meter resolution. To quantify annual climate conditions, I calculated the Z-score of the annual CWD for the year of the second fire in reburn sequences, interpolated to 30-meter resolution.

I calculated modeled composite burn index (CBI) for all first fires in a reburn sequence at 30-m resolution using the method of Parks et al. (2019). This is an explanatory variable, to

determine if the severity of the first fire affects the amount of time before the second fire. The original formulation of CBI is a post-fire, field-based metric of severity that assesses vegetation conditions one year post fire. It assesses percent mortality of vegetation of different canopy strata in the forest to create a metric of severity (Key and Benson 2006). The method of Parks et al. (2019) uses satellite-derived spectral indices of fire severity to model a raster surface of CBI.

To determine the vegetation type and associated fire regime, I used Fire Resistance Score (FRS) from Stevens et al. (2020) to represent the biological composition of the study area in a fire-relevant, functional trait-based framework. FRS reflects the functional, fire adaptive traits from different conifer tree species and where those species occur on the landscape, represented as a spatial index at 250-meter resolution. I interpolated this down to 30 meters to match the rest of the dataset.

I calculated distance to wilderness boundary (DTWB) to assess the impact of land use designation and as an indicator of likelihood of human ignition and the risk that might influence managers' decisions to suppress natural ignitions or not (Barnett et al. 2016). The southern portion of the SBW is contiguous with the northern portion of the Frank Church River of No Return Wilderness, except for the Magruder corridor, a road that runs between the two wilderness areas. I merged the two wilderness area perimeters, eliminating the boundary created by the Magruder corridor, then made a distance to perimeter layer at 30-meter resolution.

I checked for correlation of all predictor variables using "corrplot" (Wei and Simko 2021) using the Spearman correlation coefficient. The highest correlation was -0.21 between FRS and TPI; the next strongest correlation was between FRS and CWD at 0.20 (Figure A1), since correlations are considered weak, there was no close relationship to the variables, thus I retained all of them.

Statistical analysis

I used conditional inference trees (Hothorn et al. 2006) to estimate the relative importance of the topographic, climatic, biological, and geographic variables on burn history. Conditional inference trees use recursive partitioning in tree-structured regression models using conditional inference. This modeling approach avoids overfitting and variable selection bias, common problems within exhaustive search procedures applied in random forest and boosted regression trees. Overfitting and variable selection bias are avoided in this method because an ANOVA is used to determine if there is significant association between covariates and if not, recursion stops. Splitting is determined by which covariate has the largest F ratio (Hothorn et al. 2006). Conditional inference trees were grown using the "caret" package (Kuhn 2021), $\alpha = 0.05$, and a minimum of 10 observations in each branch.

I modeled fire interval using generalized linear models to look at what is causing areas to reburn at different intervals. I initially examined variables univariately and considered different transformations including quadratic, logistical, and square root. Due to the discrete nature of the response variable, I tried fitting models with a Poisson distribution as well as a negative binomial distribution. For the negative binomial distributions models, which was the distribution of the final model I fitted, I used the "MASS" package (Venables and Ripley 2002). I ranked models using Akaike information criterion (AIC) (Bozdogan 1987). All analysis was done using R (R Core Team 2021).

Results

Contemporary Fire History

Of the burnable portions (excluding perennial ice, water, and rock) of the SBW from 1985 to 2020, 11% burned twice or more, 34% burned once, and 55% did not burn (Table 1). This fire history corresponds to a 65-year fire rotation period. Large amounts of the landscape burned during times when there were high positive CWD Z-scores which are warm and dry years (Figure 2). Individual fire recurrence intervals spanned from 1 to 30 years for areas that experienced two or more fires during the study period (Figure 3). The fires that burned during the one-year intervals occurred three times with the first fire years being 1987, 2002, and 2012.

Table 1. Area occupied by different burn histories (1985-2020) in the 542,385 ha Selway-Bitterroot Wilderness study area.

Burn history (1985-2020)	Area (ha)	Area (%)
No burn	300,120	55.33%
Burned (≥1 fire)	242,265	44.67%
Once burned	184,327	33.98%
Two times burned	52,702	9.72%
Three times burned	5,020	0.93%
Fourth times burned	213	0.04%
Five times burned	3	<0.01%

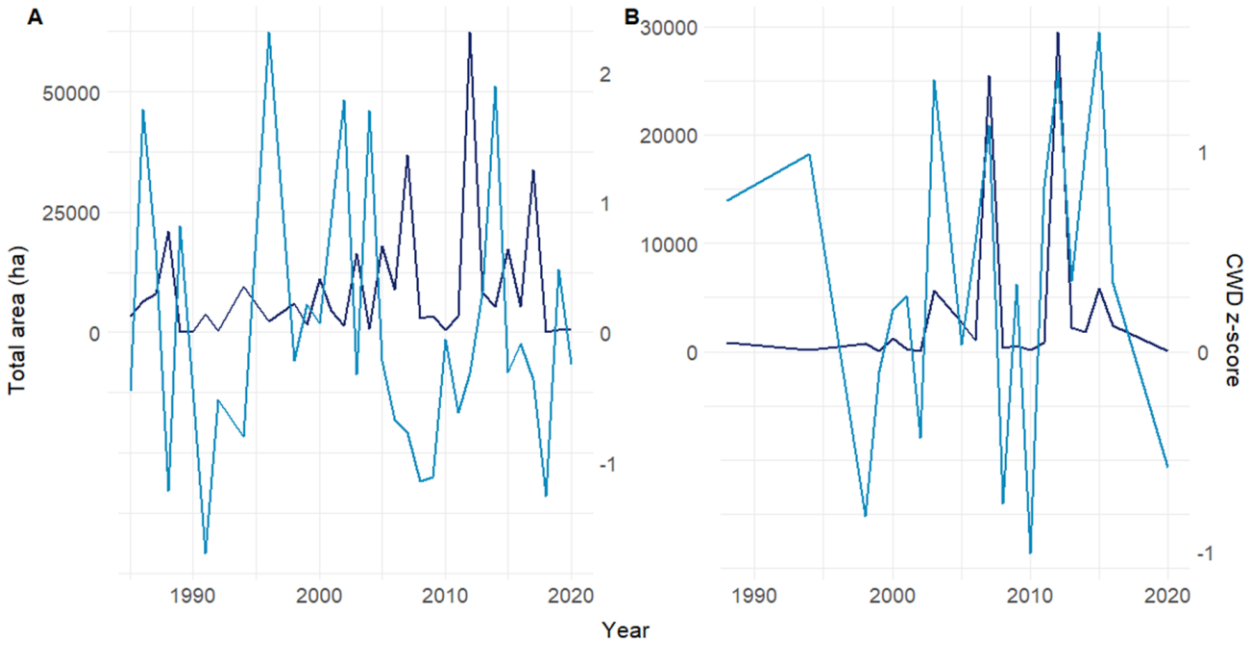

Figure 2. (A) Annual area burned in hectares from 1985 to 2020 in dark blue and Z-score of CWD in light blue. (B) Annual area reburned from 1985-2020 in dark blue and Z-score of CWD in light blue.

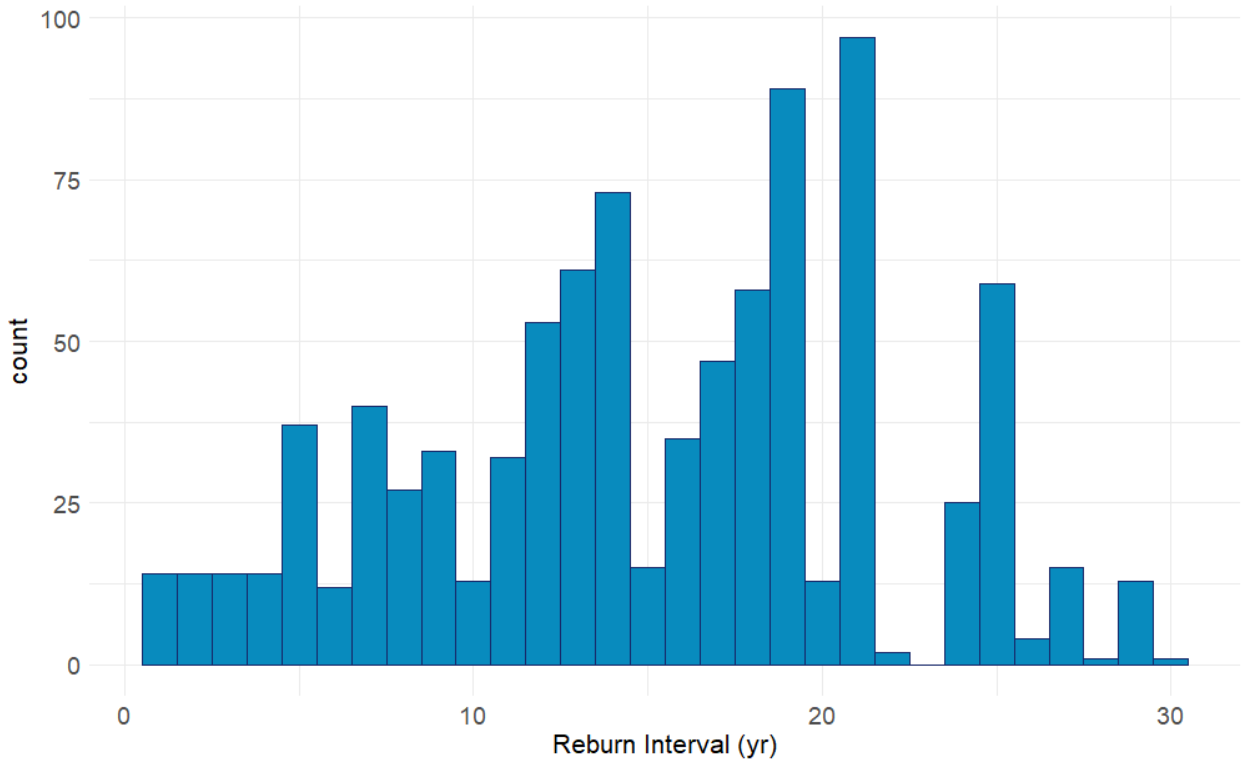

Figure 3. Frequency of fire interval (years) between first and second fire, for any 900 m^2 pixel on the landscape, from among all fires ≥ 20 ha (1985-2020).

Landscape Attributes of Different Burn Histories

These fire histories occupy different areas of the landscape climatically, topographically, in relation to political boundaries, and different community compositions (Figure 4). Mean CWD for the landscape is 179 mm and is distributed with a slight left skew (Figure 4). Areas that have not burned since 1985 tend to have lower CWD values (mean 162 mm). While areas that have burn once have slightly high CWD values (mean 173 mm) and areas have had multiple burns have even higher CWD values (mean 202 mm), with a distinctly heavier right tailed distribution relative to unburned and once-burned areas (Figure 4a).

TPI across the landscape is mostly normally distributed with a mean of 6. There is less clear separation of TPI values based on burn history. However, areas that have experienced

multiple fires tend to be mid-slope with more values around 0 TPI (mean -10), areas that have burned once are slightly more positive or upslope values (mean 16), and areas that have unburned tend to occupy more lower slope values (mean 19) (Figure 4b).

FRS and DTWB have a bimodal distribution across the landscape; however, the different burn histories depart from this pattern. A large portion of the unburned FRS distribution is centered around the 0.45 score. While once-burned areas follow the distribution of the landscape FRS distribution closely, except for a higher distribution around the 0.4 FRS. The areas with multiple burns have a more areas with lower FRS between 0.35 and 0.4 and in the higher FRS 0.47 to 0.55 than the landscape.

Distance to wilderness boundary has quite a bit of separation by burn history. Toward the edge of the wilderness boundary, there are more areas that have had no recent burns. Areas that have burned once are more abundant just a little further in and areas that have had multiple burns are most abundant in the core area of the wilderness (Figure 4c).

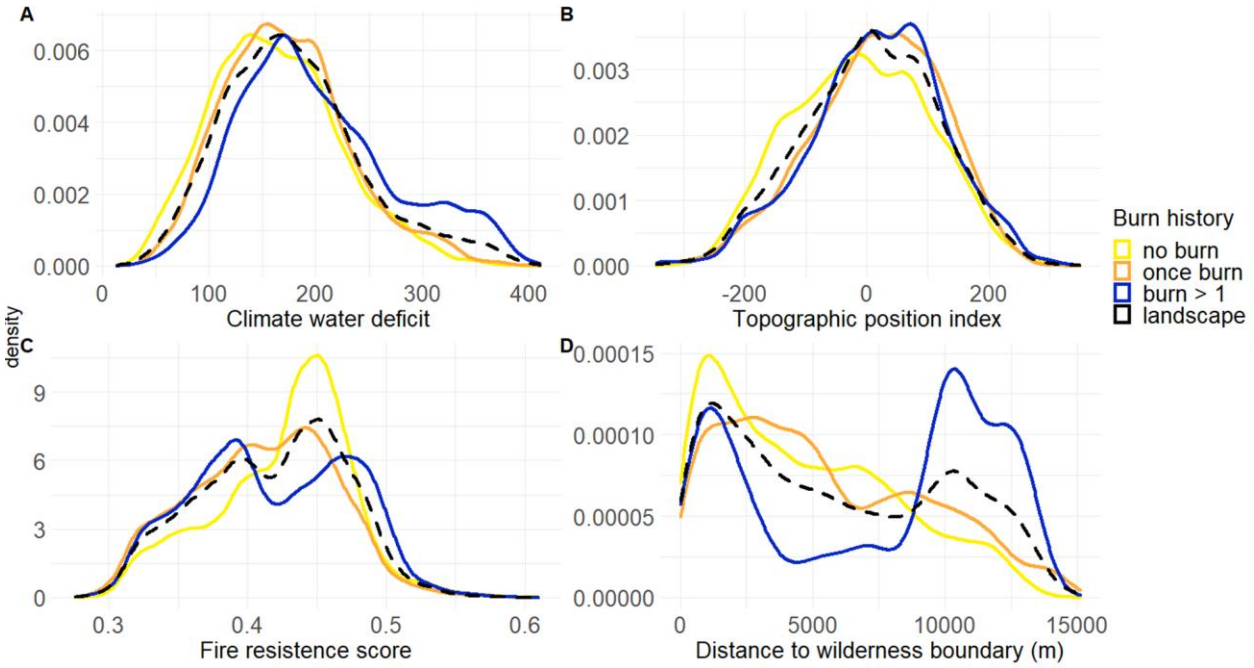

Figure 4. Density curves of: (A) climatic water deficit (CWD), (B) topographic position index (TPI), (C) fire resistance score (FRS), and (D) distance to wilderness boundary. Density curves are based on an equally sized simple random sample of from each burn history. The landscape category is a random sample of the entire burnable landscape and is shown to provide a reference expected distribution.

The conditional inference model (Figure 5) predicting the number of times burned from the explanatory variables of CWD, TPI, FRS, and DTWB had an accuracy of 54%. The first split was DTWB at 9 km. When less than 9 km, the next most important variable is FRS. In the areas less than 9 km to the wilderness boundary that had an FRS score greater than 0.425, CWD was the next most important factor. Areas with CWD less than 331 mm were more likely not have burned or burned once; while areas that had CWD greater than 331 mm were more likely to have multiple burns. In these areas further from the wilderness boundary, the next most important factor whether CWD was less than or greater than 164. If CWD was less than 164 mm, then TPI

was the most important in differentiating burn history. If TPI was less than 22 then the area was more likely to have not burned or burned once, if the area had a TPI of greater than 22 then it was more likely to have multiple fires.

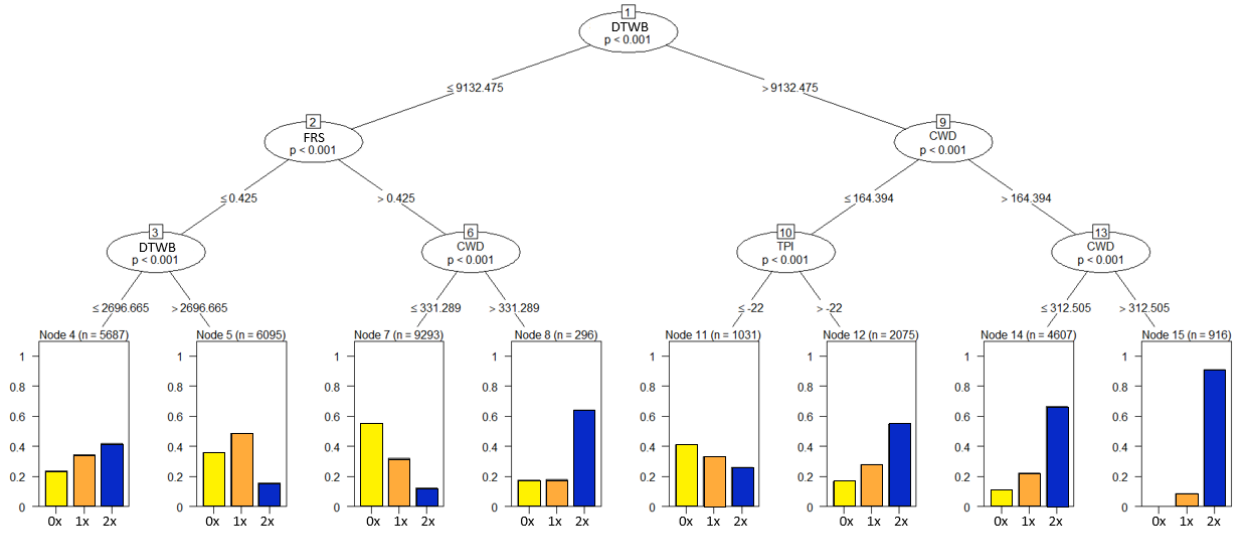

Figure 5. Conditional inference tree for different burn histories based on climatic (CWD), topographic (TPI), distance to wilderness boundary (DTWB), and biological (FRS) variables. 0x is unburn area from 1985-2020, 1x are places that burned once and 2x are areas that burned at least twice and as many as five times in the study period.

More extreme positive annual CWD (i.e., hot/dry years) was associated with longer fire intervals (Table 2; Figure 6a). TPI has a positive quadratic relationship (Z-score = -2.81) with fire interval, where fire interval is higher end ranges of TPI, lower and upper slopes, and TPI is lower at mid slopes (Table 2; Figure 6b). DTWB has a positive logarithmic relationship (Z-score = 5.85) with increasing fire interval, where fire interval is lowest closer to the wilderness boundary and fire interval is higher further into the wilderness boundary (Table 2; Figure 6c).

FRS had a logarithmic relationship with fire interval and was lowest at the more extreme high and low ranges of FRS and higher in the middle (Table 2: Figure 6d). Both CBI and the average CWD were not related to fire interval. This final model had a r^2 of 0.17.

Table 2. Results of the generalized linear model with the response variable of fire interval for the Selway-Bitterroot Wilderness, Idaho, 1985-2020.

Variable	Coefficient	Standard Error	Z-score
Annual CWD	0.19	0.03	6.59
TPI	-0.56	0.44	-1.28
TPI^2	1.09	0.43	2.51
DTWB	0.00041	0.00005	8.08
log (DTWB)	-0.18	0.04	-4.98
FR	-6.55	2.284	-2.87
log (FR)	2.80	0.95	2.9

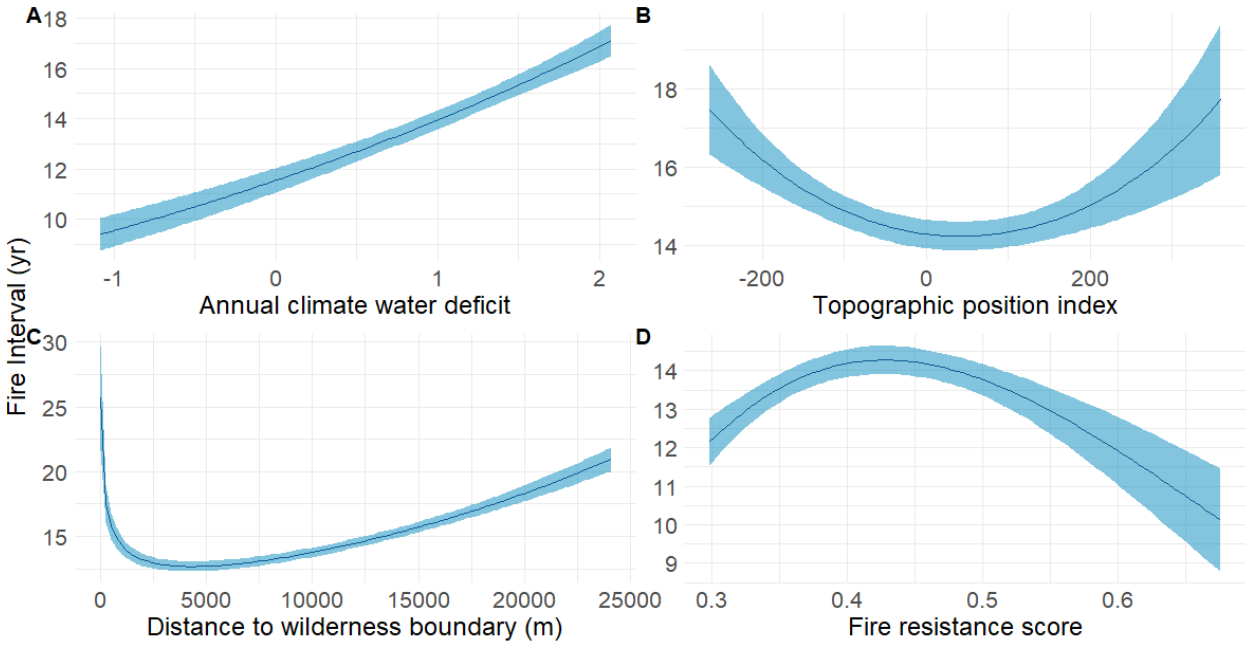

Figure 6. Partial response curves for the Generalized Linear Model of Fire Interval from 1985-2020 in the Selway-Bitterroot Wilderness, Idaho, USA. (A) Topographic position index, (B) Annual climate water deficit, (C) Distance to wilderness boundary, and (D) fire resistance score.

Discussion

Biophysical Factors Affecting Burn Histories

This study identified patterns of fire occurrence and drivers of the contemporary fire regime throughout the Selway-Bitterroot Wilderness. The varying burn histories in the SBW from 1985 to 2020 had differences in CWD, TPI, FR, and DTWB. Areas that had multiple fires tended to have the highest average CWD values, followed by areas that had burned once, and areas that had not burned tended to have the lowest CWD values (Figure 4a). As average CWD values increase, vegetation and fuels tend to be more dry and thus more readily available to burn (Stephenson 1998). These areas with high mean CWD also may be more adapted to fire regimes

with more frequent fires (Pausas and Ribeiro 2013). These areas burning more when hotter and drier which is in line with other studies in mixed-conifer forests (Cansler and McKenzie 2014)

Areas with multiple fires tended to occur around mid-slope while areas with no fire tended to occur in lower slope positions and areas with one fire tended to occur in upper slope areas. Mid-slope may have more fires because these areas tend to be more productive and thus may have more fuel accumulation (Holsinger et al. 2016, Povak et al. 2018). Lower slope positions may experience less fire if they are too moist to burn such as in riparian areas or locations that experience cold air drainage and pooling (Povak et al. 2018). Also, because this study is occurring in a wilderness, there are less anthropogenic ignitions, so the most likely way for a fire to occur is by lightning. Lightning is mostly likely to strike on ridges and areas of higher slope positions, so lower elevation areas are less likely to have an ignition (Krawchuk et al. 2009). This may also be why the areas that have burned once tend to occur in upslope areas, even though they tend to be areas with long fire return intervals.

More frequent fires were more likely to occur with increasing distance from the wilderness boundary (Figure 4c). The significant influence of DTWB (Figure 3) suggests a human influence on the fire regime even in this large, designated wilderness with a nearly 50-year history of managed wildfire (Berkey et al. 2021b, Johnston et al. 2021). Fire suppression is ubiquitous across the western United States and is even common in wilderness settings that have active fire regimes (Kreider et al. 2022). Fires are more likely to be suppressed closer to wilderness boundaries because they are more likely to escape (Barnett et al. 2016). Lower frequency of repeat fires near the boundaries of the SBW suggests an influence of suppression on the fire regime, even in this large wilderness area where fire is often managed for resource benefit.

The conditional inference analysis revealed different common characteristics of the different burn histories (Figure 5). Beyond the initial split of DTWB at 9 km, different climate and topographic variables interactions were able to explain different burn histories. The areas more than 9 km from the boundary have a lot of fire, especially in higher deficit areas. In lower deficit areas, TPI leads to a different proportion of fire history outcomes. Upper slopes are more likely to burn than lower slopes, they may be due to ignition propensity or fuel moisture (with wetter valley bottoms and drier ridges). If closer to the wilderness boundary, FRS is the next split right through the mesic shade tolerant species range at 0.425. Species in the lower end of the FRS for mesic shade-tolerant and the subalpine arid species are influenced by being within two kilometers of the wilderness boundary with areas right on the border burning more than areas more than two kilometers away. This may be caused by species composition of this area or could represent managers allowing fires from outside the wilderness area to spread across the wilderness boundary. If the FRS was more than 0.425—the upper end of the mesic shade-tolerant species and the frequent-fire associated species—CWD became very important in determining burn history. Low deficit with these less fire tolerant species has lots of unburned areas and high CWD has lots of areas with multiple burns—this is more evidence of the SBW being a climate-based fire regime. CWD is an important variable regardless of DTWB, as seen in nodes 6 and 13 (Figure 5): with high enough deficit, these areas will burn which corresponds to the right skew of the CWD distribution for the multiple burn areas (Figure 4).

Fire interval

Fire interval is affected by annual CWD, TPI, DTWB and FRS but is unrelated to average CWD and CBI. As the Z-score of annual CWD increases so does the length of the fire interval. Areas that are burning when annual CWD is higher are areas that have longer fire

intervals. These are areas with less frequent fire regimes that become available to burn during dry years. As seen in Figure 2, dry years drive large fire years with large areas burned (Morgan et al. 2008, Parisien et al. 2012, Parks et al. 2018) and are an important control for reburning, exemplifying that extreme fire weather in hot, dry years makes subalpine and moist site vegetation available to burn, and also overrides self-limitation of previous fires on subsequent fire spread.

The areas that are burning most frequently, with the shortest fire interval, are at mid-slope positions within the productive forests, with lots of fuel and a perhaps a propensity for lightning strikes. Fire interval increases at lower slope positions because there are fewer ignitions and increases at high elevations because fuel moisture is too high to support burning in most years. These higher position forests are less productive, it takes longer for fuels to accumulate and there is less time when these fuels are available for burning climatically.

Fire interval increases with increase in DTWB. After the initial drop from the perimeter, more fires overall and the occurrence of reburns is more likely in the core portion of the wilderness, the length of time between fires increases with increasing DTWB. This might have to do with the vegetation type that is reburning. Fires occurring in the mid-elevation mixed-conifer forests and high elevation subalpine forests tend to have fire return intervals longer than lower elevation more drier vegetation types.

The FRS range was 0.3-0.6, the lower end of the spectrum near 0.3 is associated with some of the less fire resistant arid subalpine species such as *Abies lasiocarpa* (Stevens et al. 2020). The scores in the middle of the range are associated with the mesic site and shade-tolerant species such as *Abies grandis, Thuja plicata, and Pseudotsuga menziesii*. The scores around 0.6 are associated with more fire-resistant species such as *Pinus monticola and Larix occidentalis*.

Pinus ponderosa (FRS = 0.77) is a frequent-fire conifer that was present in the SBW but not represented in the FRS range because FRS is a community level estimate that comes from a mixture of species with different fire resistance traits. Fire interval was shorter in the fire resistant arid subalpine species as well as in the frequent-fire associated species and longer in the mesic shade-tolerant species. It is intuitive that there would be a shorter fire interval in the communities composed of frequent-fire associated species. The subalpine species one would initially hypothesize would have a longer fire interval; however, the time period of this study was very warm and dry relative to the long-term average climate (Morgan et al. 2008, Higuera et al. 2015). This being a climate driven fire regime increased the propensity for these areas that typically have long historical average fire return intervals to have a shorter individual fire intervals during the study period. The mesic shade tolerant species typically inhabit a mixed-conifer forest, mixed-severity fire regime, and mid-slope areas. They are less impacted by variations in climate compared to their higher elevation counterparts.

Fire is impacted by climatic, topographic, biological, and anthropogenic factors. More area burning during the warm and dry periods leads to the conclusion of a climate, rather than fuel limited ecosystem. The increase in area burned and reburned during the warm dry years (Figure 2), shows that this is a climate limited fire regime (Krawchuck and Moritz 2011, Pausas and Paula 2012).

Conclusion

Bettering understanding of when and where fires are occurring on the landscape and what is causing certain areas to burn more gives us a deeper understanding of the fire regime in the SBW and in the northern Rocky Mountains, and how it may change in the future. The areas that are lower probability of burning are cooler and wetter, above or below mid-slope, and closer the wilderness boundary. Areas that have burned multiple times tend to be warmer and drier at mid-slope and in the core of the wilderness. The areas that have burned once are in between these two extremes. The major drivers of increased fire interval were TPI, annual CWD, and DTWB. As areas experience more frequent warmer and dry fire seasons they will burn more regardless of what the long-term average CWD (Parks and Abatzoglou 2020). This fire regime is climate driven and previous burn severity fuels are less important than the annual climate for determining how frequently an area will burn (Westerling 2016). However, beyond distances of about nine kilometers from the wilderness boundary climatic and topographic variables had stronger influence on fire frequency, suggesting hierarchal control of fire management decisions on other fire regime drivers in the SBW.

It is essential that we understand what is causing areas to burn and what is causing them to burn more often because as fires are predicted to increase in both size (Schoennagel et al. 2017) and severity (Abatzoglou et al. 2017) in the western U.S., more area previously burned will be burning again in shorter intervals.

Literature Cited

Abatzoglou, J. T., C. A. Kolden, A. P. Williams, J. A. Lutz, and A. M. S. Smith. 2017. Climatic influences on interannual variability in regional burn severity across western US forests. International Journal of Wildland Fire 26:269–275.

Arno, S. F. 1976. The Historical Role of Fire on the Bitterroot National Forest. Department of Agriculture, Forest Service, Intermountain Forest and Range Experiment Station.

Balch, J. K., B. A. Bradley, J. T. Abatzoglou, R. C. Nagy, E. J. Fusco, and A. L. Mahood. 2017. Human-started wildfires expand the fire niche across the United States. Proceedings of the National Academy of Sciences 114:2946–2951.

Barnett, K., C. Miller, and T. J. Venn. 2016. Using Risk Analysis to Reveal Opportunities for the Management of Unplanned Ignitions in Wilderness. Journal of Forestry 114:610–618.

Berkey, J. K., C. Miller, and A. J. Larson. 2021. A history of wilderness fire management in the Northern Rockies. Page RMRS-GTR-428. U.S. Department of Agriculture, Forest Service, Rocky Mountain Research Station, Fort Collins, CO.

Boisramé, G. F. S., S. E. Thompson, M. Kelly, J. Cavalli, K. M. Wilkin, and S. L. Stephens. 2017. Vegetation change during 40years of repeated managed wildfires in the Sierra Nevada, California. Forest Ecology and Management 402:241–252.

Bozdogan, H. 1987. Model selection and Akaike's Information Criterion (AIC): The general theory and its analytical extensions. Psychometrika 52:345–370.

Cansler, C. A., and D. McKenzie. 2014. Climate, fire size, and biophysical setting control fire severity and spatial pattern in the northern Cascade Range, USA. Ecological Applications 24:1037–1056.

Collins, B. M., J. D. Miller, A. E. Thode, M. Kelly, J. W. van Wagtendonk, and S. L. Stephens. 2009. Interactions Among Wildland Fires in a Long-Established Sierra Nevada Natural Fire Area. Ecosystems 12:114–128.

Krawchuk, M.A., and M.A. Moritz. 2011. Constraints on global fire activity vary across a resource gradient. Ecology 92:121-132.

Pausas, J.G., and S. Paula. 2012. Fuel shapes the fire–climate relationship: evidence from Mediterranean ecosystems. Global Ecology and Biogeography 12:1074-1082.

Habeck, J. R., and R. W. Mutch. 1973. Fire-Dependent Forests in the Northern Rocky Mountains. Quaternary Research 3:408–424.

Hessburg, P. F., C. L. Miller, S. A. Parks, N. A. Povak, A. H. Taylor, P. E. Higuera, S. J. Prichard, M. P. North, B. M. Collins, M. D. Hurteau, A. J. Larson, C. D. Allen, S. L. Stephens, H. Rivera-Huerta, C. S. Stevens-Rumann, L. D. Daniels, Z. Gedalof, R. W. Gray, V. R. Kane, D. J. Churchill, R. K. Hagmann, T. A. Spies, C. A. Cansler, R. T. Belote, T. T. Veblen, M. A. Battaglia, C. Hoffman, C. N. Skinner, H. D. Safford, and R. B. Salter. 2019. Climate, Environment, and Disturbance History Govern Resilience of Western North American Forests. Frontiers in Ecology and Evolution 7.

Higuera, P. E., J. T. Abatzoglou, J. S. Littell, and P. Morgan. 2015. The Changing Strength and Nature of Fire-Climate Relationships in the Northern Rocky Mountains, U.S.A., 1902-2008. PLOS ONE 10:e0127563.

Holling, C. S. 1973. Resilience and Stability of Ecological Systems. Annual Review of Ecology and Systematics 4:1–23.

Holsinger, L., S. A. Parks, and C. Miller. 2016. Weather, fuels, and topography impede wildland fire spread in western US landscapes. Forest Ecology and Management 380:59–69.

Hothorn, T., K. Hornik, and A. Zeileis. 2006. Unbiased Recursive Partitioning: A Conditional Inference Framework. Journal of Computational and Graphical Statistics 15:651–674.

Johnston, J. D., J. B. Kilbride, G. W. Meigs, C. J. Dunn, and R. E. Kennedy. 2021. Does conserving roadless wildland increase wildfire activity in western US national forests? Environmental Research Letters 16:084040.

Key, C. H., and N. C. Benson. 2006. Landscape Assessment (LA):55.

Krawchuk, M. A., M. A. Moritz, M.-A. Parisien, J. V. Dorn, and K. Hayhoe. 2009. Global Pyrogeography: the Current and Future Distribution of Wildfire. PLOS ONE 4:e5102.

Kreider, M. R., M. R. Jaffe, J. K. Berkey, S. A. Parks, and A. J. Larson. 2022. A review of the scientific contributions enabled by wilderness fire management. preprint, In Review.

Kuhn, M. 2021. caret: Classification and Regression Training.

LANDFIRE. 2016. Existing Vegetation Type (EVT) CONUS. U.S. Department of the Interior, Geological Survey, and U.S. Department of Agriculture.

Larson, A. J. 2016. Introduction to the Article by Elers Koch: The Passing of the Lolo Trail. Fire Ecology 12:1–6.

Morgan, P., E. K. Heyerdahl, and C. E. Gibson. 2008. MULTI-SEASON CLIMATE SYNCHRONIZED FOREST FIRES THROUGHOUT THE 20TH CENTURY, NORTHERN ROCKIES, USA. Ecology 89:717–728.

Parisien, M.-A., S. Snetsinger, J. A. Greenberg, C. R. Nelson, T. Schoennagel, S. Z. Dobrowski, M. A. Moritz, M.-A. Parisien, S. Snetsinger, J. A. Greenberg, C. R. Nelson, T. Schoennagel, S. Z. Dobrowski, and M. A. Moritz. 2012. Spatial variability in wildfire probability across the western United States. International Journal of Wildland Fire 21:313–327.

Parks, S. A., and J. T. Abatzoglou. 2020. Warmer and Drier Fire Seasons Contribute to Increases in Area Burned at High Severity in Western US Forests From 1985 to 2017. Geophysical Research Letters 47:e2020GL089858.

Parks, S. A., L. M. Holsinger, M. J. Koontz, L. Collins, E. Whitman, M.-A. Parisien, R. A. Loehman, J. L. Barnes, J.-F. Bourdon, J. Boucher, Y. Boucher, A. C. Caprio, A. Collingwood, R. J. Hall, J. Park, L. B. Saperstein, C. Smetanka, R. J. Smith, and N. Soverel. 2019. Giving Ecological Meaning to Satellite-Derived Fire Severity Metrics across North American Forests. Remote Sensing 11:1735–1735.

Parks, S. A., L. M. Holsinger, C. Miller, and C. R. Nelson. 2015a. Wildland fire as a self-regulating mechanism: the role of previous burns and weather in limiting fire progression. Ecological Applications 25:1478–1492.

Parks, S. A., L. M. Holsinger, C. Miller, and C. R. Nelson. 2015b. Fire atlas for the Selway-Bitterroot Wilderness. Forest Service Research Data Archive.

Parks, S. A., M.-A. Parisien, C. Miller, L. M. Holsinger, and L. S. Baggett. 2018. Fine-scale spatial climate variation and drought mediate the likelihood of reburning. Ecological Applications 28:573–586.

Pausas, J. G., and E. Ribeiro. 2013. The global fire–productivity relationship. Global Ecology and Biogeography 22:728–736.

Povak, N. A., P. F. Hessburg, and R. B. Salter. 2018. Evidence for scale-dependent topographic controls on wildfire spread. Ecosphere 9:e02443.

R Core Team. 2021. R: A language and environment for statistical computing. R Foundation for Statistical Computing. Vienna, Austria.

Schoennagel, T., J. K. Balch, H. Brenkert-Smith, P. E. Dennison, B. J. Harvey, M. A. Krawchuk, N. Mietkiewicz, P. Morgan, M. A. Moritz, R. Rasker, M. G. Turner, and C. Whitlock. 2017. Adapt to more wildfire in western North American forests as climate changes. Proceedings of the National Academy of Sciences 114:4582–4590.

Steel, Z. L., H. D. Safford, and J. H. Viers. 2015. The fire frequency-severity relationship and the legacy of fire suppression in California forests. Ecosphere 6:art8.

Stephenson, N. 1998. Actual evapotranspiration and deficit: biologically meaningful correlates of vegetation distribution across spatial scales. Journal of Biogeography 25:855–870.

Stevens, J. T., M. M. Kling, D. W. Schwilk, J. M. Varner, and J. M. Kane. 2020. Biogeography of fire regimes in western U.S. conifer forests: A trait-based approach. Global Ecology and Biogeography 29:944–955.

Venables, W. N., and B. D. Ripley. 2002. Modern Applied Statistics with S. Fourth. Springer, New York.

Wei, T., and V. Simko. 2021. R package "corrplot": Visualization of a Correlation Matrix.

Weiss, A. D. 2001. Topographic position and landforms analysis. San Diego, CA.

Westerling, A. L. 2016. Increasing western US forest wildfire activity: sensitivity to changes in the timing of spring. Philosophical Transactions of the Royal Society B: Biological Sciences 371:20150178.

Wilson, J. P., and J. C. Gallant, editors. 2000. Terrain Analysis: Principles and Applications. Pages 87–131 Secondary Topographic Attributes. Wiley, New York.

Appendix A.

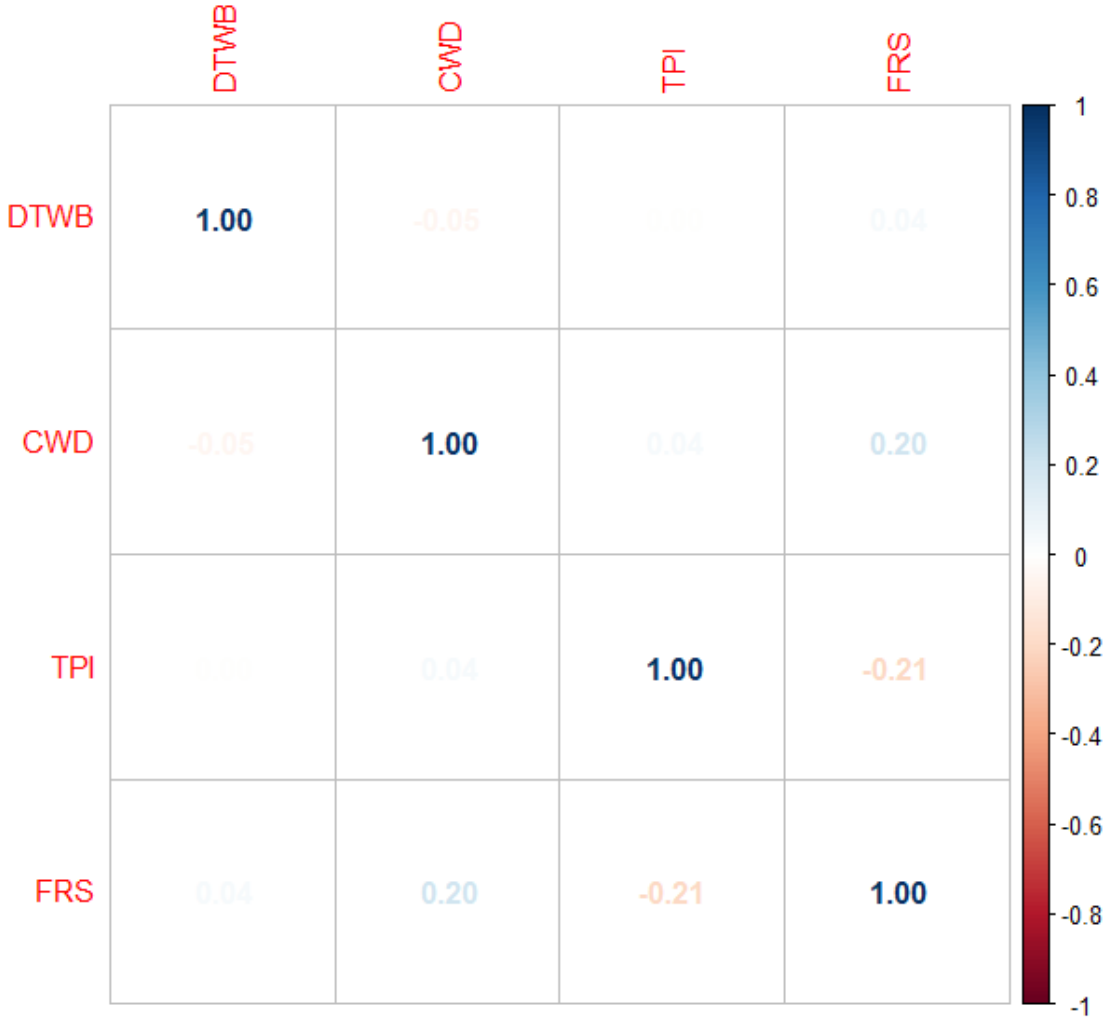

Figure A1. Correlation plot of all explanatory variables in the of the conditional inference model.

Chapter 2: The legacy of historical high-severity fire in the Selway-Bitterroot Wilderness

Abstract

High-severity fires create lasting effects on landscape vegetation mosaics. Recent increases in fire activity and severity highlight the need to understand the long-term effects of high-severity fire, including interactions with subsequent fires. In the northern US Rocky Mountains, including Selway-Bitterroot Wilderness (SBW), the early 20th century saw several years marked by large, high-severity fires. I investigated the influence of fire frequency (once, twice, and thrice burned from 1910-2017) on forest structure, conifer regeneration, and fuel loading in areas that initially burned at high severity in the SBW in 1910 or 1934. I found that 129,682 hectares of mixed-conifer forest burned during regional fire years between 1910-1934. Of that area, 38,014 hectares reburned once and 3999 hectares reburned twice between 1985 and 2017. Conifer tree regeneration was abundant across all three burn histories and 99% of sample sites were <200 m from the nearest seed source. Douglas-fir seedling density was higher in areas that burned two or three times; grand fir seedlings was more abundant in once-burned areas. Snags and coarse woody material were less affected by fire frequency and more impacted by having a recent (since 1985), second or third fire. High shrub biomass only occurred on steep southwest aspects with low overstory tree basal area and was not related to fire history. Live tree composition and density differ across forests that initiated from early 20th century high-severity fire with contrasting recent fire history, but even thrice-burned sites are largely regenerating to forest communities.

Introduction

High-severity fires create a lasting effect on the landscape vegetation mosaic. Recent area burned and proportion of area burned at high-severity have increased throughout the western United States (Abatzoglou and Williams 2016a, Parks and Abatzoglou 2020a, Hessburg et al. 2021). This raises the question of how these areas may develop after fire, and what the long-term legacy will be in terms of both the development of burned sites, as well as the interactions with future disturbances. However, this is not the first time that high-severity fires have been widespread on the landscape. In the early twentieth century there were many climate and weather driven regional fire years (Brunelle et al. 2005, Morgan et al. 2008c) with large areas burned at high severity across the northern Rocky Mountains.

Fire alters vegetation structure and composition, as well as fuel type and amount (Tepley et al. 2018). Early 20th century high-severity fires in the northern Rocky Mountains reset succession and impacted the trajectory of vegetation development (Larsen 1925). These alterations create a legacy on the landscape and, in turn, affect the probability and pattern of future fire severity and spread (Parks et al. 2015a), as well as the potential successional trajectory of the vegetation. Post-fire fuel loads and structure can directly impact subsequent fires behavior and effects (Stevens-Rumann and Morgan 2016).

Reburns are burned areas that have burned previously within a specified temporal window. Reburns modify patterns and affect subsequent fires (Prichard et al. 2017) creating unique fuel and vegetation compositions and structures (Stevens-Rumann and Morgan 2016, Ward et al. 2017), which potentially shift successional trajectories and influence the spread and intensity of future fires (Kipfmueller and Kupfer 2005, Busby et al. 2020). Short-interval fires, with a fire-return interval less than about 30 years, are well studied (Larson et al. 2013, Parks et al. 2014, 2018, Stevens-Rumann and Morgan 2016, Prichard et al. 2017, Berkey et al. 2021a).

Similarly, extensive research has been conducted on long-interval fires, mostly through tree ring reconstruction of fire history and stand development, and with chronosequence and long-term studies of forest stand dynamics (Huff 1995, Taylor 2000, Taylor and Skinner 2003, Van Pelt et al. 2004, Larson et al. 2008). However, less fire history and forest structure research has been done from an a priori rather than opportunistic approach on this timescale, where the time and severity of the initial fire in a fire history sequence is known before sampling rather than reconstructed and inferred from tree ring records.

Warming caused by anthropogenic climate change continues to alter fire regimes in the western US. Shifting fire regimes can have significant effects on forest structure and composition. This can reduce resilience, leading to reduced regeneration for some tree species (Davis et al. 2020) and changes in dominant vegetation type (Coop et al. 2020). As fires are predicted to increase in both size (Schoennagel et al. 2017) and severity (Abatzoglou et al. 2017) in the western U.S., more area previously burned may burn again with shorter intervals. It is thus essential to understand the impact of different fire sequences on forest structure and developmental trajectories (Abatzoglou and Williams 2016b, Littell et al. 2018, Parks and Abatzoglou 2020b).

Early 20th century high-severity fires burned prior to widespread fire suppression and exclusion. Thus, they are useful as model systems in which to investigate of the long-term effects of high-severity fires that burned in an active, minimally altered fire regime. Figure 1A shows an area that experienced high-severity fire in 1910 about 20 years after the 1910 fires. In areas with the potential to be forests, there is a mosaic of forested and non-forested areas. Forest area and density increased in the mid-twentieth century with policy changes, such as the implementation of widespread fire suppression as with the 10 AM policy, and with climate being cooler and

wetter (Hessburg et al. 2015). This phenomenon can be seen in Figure 1B, showing the fire perimeter 60 years after the initial high-severity fire. Change in wilderness fire policy and climate created more area burned from late twentieth century to present day (Berkey et al. 2021), creating opportunities for some portions of the original fire perimeter to reburn (Figure 1C). While other areas of the original burn, that have not reburned, continue to follow the trend of forest regeneration and increasing density.

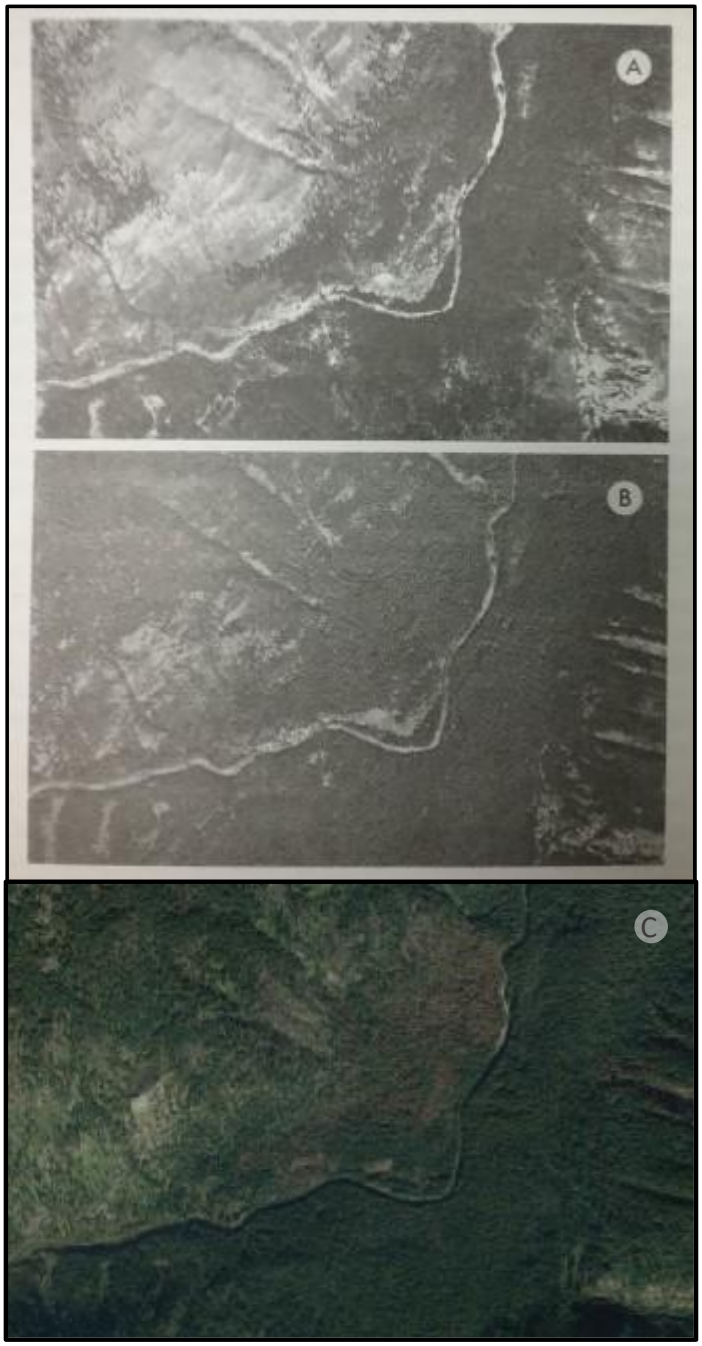

Figure 1. Aerial photos of the Elbow Bend area of the East Fork of Moose Creek, Selway-Bitterroot Wilderness, Idaho, USA. (A) 1939 photo depicting extensive brush fields that developed following the 1910 fire. (B) 1970 photo depicts forest invasion of the upland slopes (Habeck 1976). (C) 2017 image from Google Earth showing the same area.

Many studies have looked the effects of a single reburn, that is, areas having burned twice in the time interval in question (e.g., Stevens-Rumann and Morgan 2016, Prichard et al. 2017, Hoecker and Turner 2022). Yet, there has been relatively little research discerning differences between once-, twice-, and thrice-burned areas. Furthermore, long-term studies of forest development following a fire of known origin date and severity that include interactions with subsequent reburns are rare. Most reburn literature investigates the period since the development of satellite imagery to characterize fire events (1972) there is little use of information about pre-1972 conditions.

Here, I investigate the influence of different fire histories on forest fuel, composition, and structure in patches that initially burned at high severity in the early 20th century. I focus on these years as they are important climate and weather driven fire events that occurred before the widespread effects of fire suppression and are typical of the conditions in which large areas burn regionally (Morgan et al. 2008). Specifically, I study how forest structure and composition, tree regeneration, and fuels differ in areas burned once, twice, and thrice with an initial high-severity fire.

Methods

Study Area

I conducted my research in the Moose Creek Ranger District in Selway-Bitterroot Wilderness (SBW) (Figure 2). The SBW is a 545,372 ha congressionally designated wilderness area situated in western Montana and north central Idaho, USA. The Moose Creek Ranger District makes up 226,623 hectares of the SBW, west of the Bitterroot Range and south of the Lochsa River. The elevational range of the SBW is 531 m to 3,096 m and it has a mean annual precipitation 1221 mm and a mean annual temperature of 3.5°C (Parks et al. 2015a). Low and

middle elevation forests I sampled in the SBW are composed of (*Pinus ponderosa*) and Douglas-fir (*Pseudotsuga menziesii*) on warm and dry sites, with variable mixtures of western redcedar (*Thuja plicata*), grand fir (*Abies grandis*), western white pine (*Pinus monticola*), and Engelmann spruce (*Picea engelmannii*) on mesic sites. (Finklin 1983, Rollins et al. 2000, Berkey et al. 2021a).

I used the LANDFIRE Existing Vegetation TYPE (EVT) (LANDFIRE 2016) to locate the areas I was interested in sampling: mid-elevation, mixed-conifer forests. I removed all non-forested, ponderosa pine savanna, and subalpine forest types. The vegetation types that were left after masking by forest type were: Northern Rocky Mountain Dry-Mesic Montane Mixed Conifer Forest and Northern Rocky Mountain Mesic Montane Mixed Conifer Forest. This ensured that the areas had the capacity to produce forests and being mid-elevation and the same species type reduced variability. I also constrained my sampling by severity of the first fire: all initial fires had to be high severity and to have occurred in regional fire years as defined by Morgan et al. (2008b). Regional fire years of the early 20th century were 1910, 1919, 1926, 1929, 1931, and 1934 for the Northern Rockies. The SBWs regional fire years were 1910, 1919, and 1934. These are the years where area burned exceeded the 90th percentile of annual fire extent (Morgan et al. 2008). I created an interior buffer of 200 m of the original fire perimeter, meaning I removed the exterior 200 m of area of the original fire perimeters to assure that when sampling we were in the actual early 20th century fires and were not affected by potential nominal GPS error or edge effects. The initial high-severity fires could not have burned from 1870 (the beginning of the dataset) until initial high-severity fire in the early twentieth century. These fires could have only burned up to three times and the reburns occurred in the modern period, after 1979. The most recent fire could not have burned after 2017, giving time for the area to recovery

and begin a post-fire successional trajectory. The first, second and third fire all had to be within the same watershed and close to contiguous in any sampling block. Given these constraints, the final sites selected for sampling had initial fire years of 1910 and 1934.

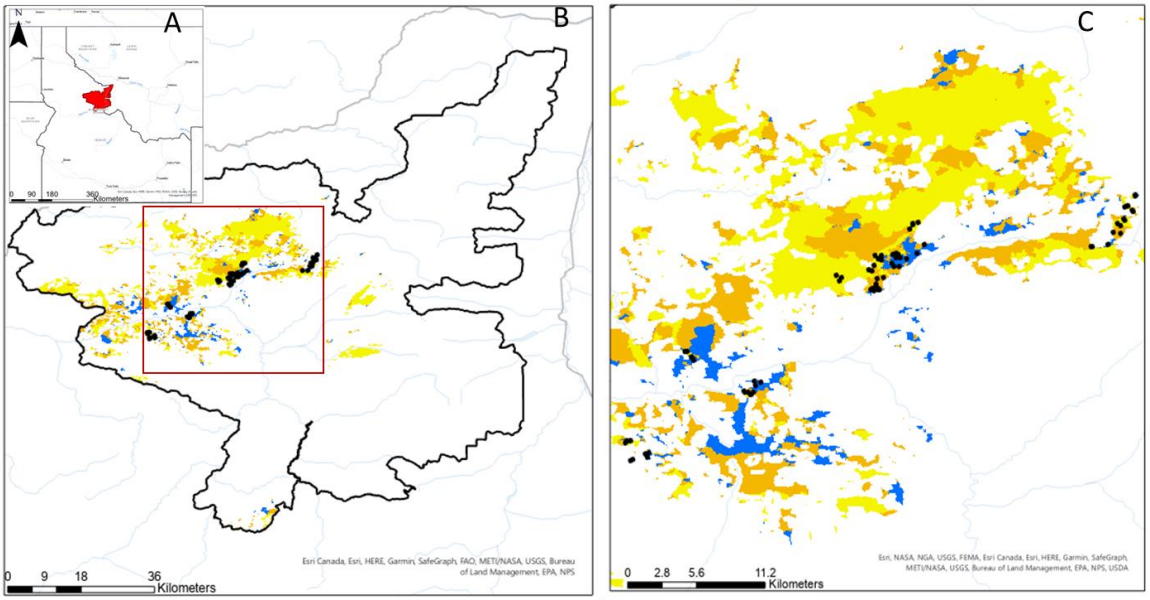

Figure 2. The location of the study. (A) Location of the Selway-Bitterroot Wilderness (SBW) within the western United States. (B) The study area location within the SBW and the fire perimeters of high-severity fires that burned in either 1910 or 1934 and have been buffered inward 120 m to ensure sample site is in historical fire area. (C) Inset of all the plots with burn history.

Fire history records and sample design

I created a fire atlas of burn perimeters and fire severity for the SBW for 1870-2020. To do this I combined two datasets: a historical dataset of fire perimeters and severity from 1870-2000 created by Pat Green, retired US Forest Service Ecologist (Morgan et al. 2014); and dataset of fire perimeters from 1972-2015 and satellite derived severity metrics (Parks et al. 2015c), which I extended using similar methods for the years 2016-2020. The Green dataset contains fire perimeters and fire severity patches (high, moderate, low) delineated by hand and determined by photo-interpreted evaluation of tree mortality (Morgan et al. 2014). The Parks dataset was generated from fire perimeters identified with satellite derived imagery (Parks et al. 2015c).

To identify areas that burned at high severity in the early 1900's for field sampling, I combined the Green and Parks datasets into a single fire occurrence and severity atlas including verification that high-severity classification was comparable among the two datasets (Appendix A). I calculated severity for the Parks et al. (2015a) using composite burn index (CBI) (Key and Benson 2006) from remote sensing imagery using methods and code from Parks et al. (2019). Then, I determined what CBI cut-off corresponded to a high-severity classification in the Green dataset. Using a moving window summary, I smoothed the satellite derived severity to make the patch size and composition similar to that of the Green dataset. I created binary classifications of high-severity and non-high-severity for the smoothed raster. I then created an interior buffer of 120 m (4 pixels) creating core high-severity patches to reduce the likelihood of potential projection or delineation error that may have occurred in the creation of the Green dataset (Appendix A).

I used only regional fire years for the first fires in the early twentieth century (1910, 1919, 1926, 1929, 1931, 1934) to ensure large sample sizes and increase confidence in the dates of historical fire (Morgan et al. 2008c). I ensured that the areas had not burned since 1870 to our

regional fire in the early twentieth century. Reburns during the modern period (when LANDSAT began) occurring between 1985 and 2018 were considered for field sampling. A most recent fire of 2017 provided at least three years for post-fire tree regeneration to establish prior to field sampling.

I identified adjacent areas with the target fire history–areas that had been burned once, twice, and three times—hereafter referred to as block. I then randomly selected three sample points in each fire history patch for a total of nine plot locations per block. I sampled nine blocks with nine plots per block, for a total of 81 plots. I ensured that it was feasible to reach each plot and that they were on a slope of 30° or less for safety through an office review of satellite imagery and slope layers.

Field measurements

At the center of each plot, I recorded location using submeter GPS, as well as slope, aspect, elevation, distance to nearest conifer seed tree, and photos of the plot. I recorded tree species, diameter at breast height (DBH), and mortality status on mature trees ($\geq$ 10 cm DBH) within a 17.84 m fixed radius of plot center. Saplings were small trees (>1.37 m tall and < 10 cm DBH) for which I recorded species, DBH in bins of 2.5 cm, and mortality status within a 5.64 m fixed radius plot around plot center. A transect oriented at a random azimuth was used to sample tree seedlings, canopy cover, ground fuels, fine fuels, and live fuels. Seedlings were censused within a 2 m by 20 m plot (1 m on either side of the central transect). I collected seedling species, mortality status, and height (within 40 cm height classes). First year seedlings were not recorded to reduce chance of biased seedling density estimates resulting from high seedling mortality during the first growing season. Canopy cover was assessed using a line intercept method with a densitometer (GRS densitometer) at one meter intervals along the transect from 2-22 m to

determine presence or absence of any biomass over 183 cm tall. At 6 m, 11 m, 16 m, and 21 m along the transect, litter and duff depth were measured by excavating to bare mineral soil and measured depth to the nearest mm with a ruler. Fine woody surface fuels and live fuels (herbs and shrubs) were measured using the photoload method (Keane and Dickinson 2007) with 1 m^2 microplots located at 6 m, 11 m, 16 m, and 21 m along the transect for a total of four microplots per plot. Coarse woody material (CWM) are 1000-hour fuels (diameter > 7.62 cm) with no minimum length. CWM was measured within a 100 m^2 (10 m × 10 m) plot, where the plot was in a random position with the left side of the quadrat (viewed from plot center) positioned clockwise to the seedlings/fuels transect. I measured all CWM small and large end diameters as well as length and decay class. If there were more than ten CWM pieces, I estimated diameters and length. I also measured canopy fuel height, recording the average crown base height and lowest crown base height (Lutes et al. 2006).

Data reduction and analysis

All measured forest structure and fuels variables were summarized at the plot level. I took an average of the four litter and duff measurements taken within the plot. CWM was converted from diameters of small and large end and length to volume using the Smalian method (Filho et al. 2000). All other woody fuels were originally measured in kg/m^2 (Keane and Dickinson 2007). Live and dead tree basal area, CWM, seedlings, and saplings were expanded to a per hectare units.

I calculated topographic wetness index (TWI) using "RSAGA" package (Brenning et al. 2018) and heat load (Welty 2018) using a Digital Elevation Model (DEM) and actual plot locations measured in the field with Juniper Systems, Geode GNSS receiver. TWI and heat load are important environmental covariates that could confound the main effect of fire frequency

(Heyerdahl et al. 2001, Meigs et al. 2020). TWI is a measurement of topographic convergence that predicts net incoming and outgoing drainage (Beven and Kirkby 1979). Heat load is an adjusted version of solar radiation that is calculated from latitude, aspect, and slope; it accounts for south-west facing slopes being warmer (higher heat load values) than north-east facing slopes (lower heat load values) (McCune and Keon 2002).

To account for the nested nature of my data, plots within fire history patches within blocks, I used linear mixed models (Zuur et al. 2009). I used a linear mixed model using the "nlme" package (Pinheiro et al. 2022) to determine the importance of frequency of fire on live tree basal area (BA) and dead tree (snag) basal area, CWM, herb load, and shrub load. My fixed effects explanatory variables were burn, block, TWI, and heat load. My random effect variable was block by burn (Block:Burn). This created a GLMM with a random intercept; I did this because it accounts for variability at the plot or block level and potential different relationships between block and fire frequency and plot and fire frequency (Zuur et al. 2009). I ranked potential models using Akaike information criterion (AIC) (Eilers and Marx 1996). All response variables were square root transformed. To further understand the herb and shrub load data I conducted quantile regression using the "quantreg" package (Koenker 2021) for both shrubs and herbs.

Principal Component Analysis (PCA) was conducted using forest structure, fuels, and regeneration data (Figure B1) to visualize and explore the relationship between fire frequency and forest structure, composition, and fuel load in multivariate space. The variables included in the PCA were: one-hour, ten-hour, hundred-hour fuels, litter depth, duff depth, CWD volume per ha, seedlings per ha, quadratic mean diameter, herb load, shrub load, live tree basal area, snag basal area, overstory tree QMD, and saplings per ha (Figure B1). The data matrix had eighty-one

rows, one for each plot, and fourteen columns. I checked correlation of variables using "corrplot" (Wei and Simko 2021). The PCA used centered and scaled values. I plotted treatment and control centroids and the directions of variables on the PCA for interpretation.

Results

Live trees and tree seedlings

There were six species of mature live trees present in the sites: *Abies grandis* (grand fir), *Picea engelmannii* (Engelmann spruce), *Pinus contorta* (lodgepole pine), *Pinus ponderosa* (ponderosa pine), *Pseudotsuga menziesii* (Douglas-fir), and *Thuja plicata* (red cedar). Forty-six percent of overstory trees were *Abies grandis* (stem basis). The second most abundant species was *Pseudotsuga menziesii,* making up 33% of total composition. *Thuja plicata*, *Pinus ponderosa Picea engelmannii*, *Pinus contorta* were 10%, 8%, 2%, <1% of stems, respectively. *Abies grandis* was more abundant in the once-burned sites compared to the reburns. Almost all *Picea engelmannii* was present in once-burned sites. *Pinus contorta* was quite rare, though a few were found in the thrice-burned areas. *Pinus ponderosa* was more abundant in the reburns, specifically the three-times burned. *Pseudotsuga menziesii* was most abundant in the twice-burned sites. *Thuja plicata* occurred most frequently in the once-burned sites (Table A4).

Live tree basal area decreased (P = 0.07) with increasing fire frequency (Figure 3; Table 1). Live tree basal area was inversely related to heat load (P = 0.02, Table 1), basal area decreased with increasing heat load and fire frequency (Figure 3C). Once-burned sites had a mean basal area of 32.1 m^2/ha while twice- and thrice-burned had a mean basal area of 21.1 m^2/ha and 14.2 m^2/ha, respectively. The diameter distribution of trees was largely populated by smaller trees, with fewer smaller trees in the sites that have reburned (Figure 3). The average

diameter of the trees for once-, twice-, and thrice-burned areas was 26 cm, 32 cm, 29 cm, respectively. Live tree basal area was not related to TWI (Table 1).

Table 1. ANOVA tables √Live Basal area GLMM with the important explanatory variables and their associated F- and p-values. The positive and negative signs denote the sign of the coefficient.

Variable	F-value	p-value
Fire frequency (-)	3.25	0.07
TWI	0.04	0.83
Heat load (-)	5.50	0.02

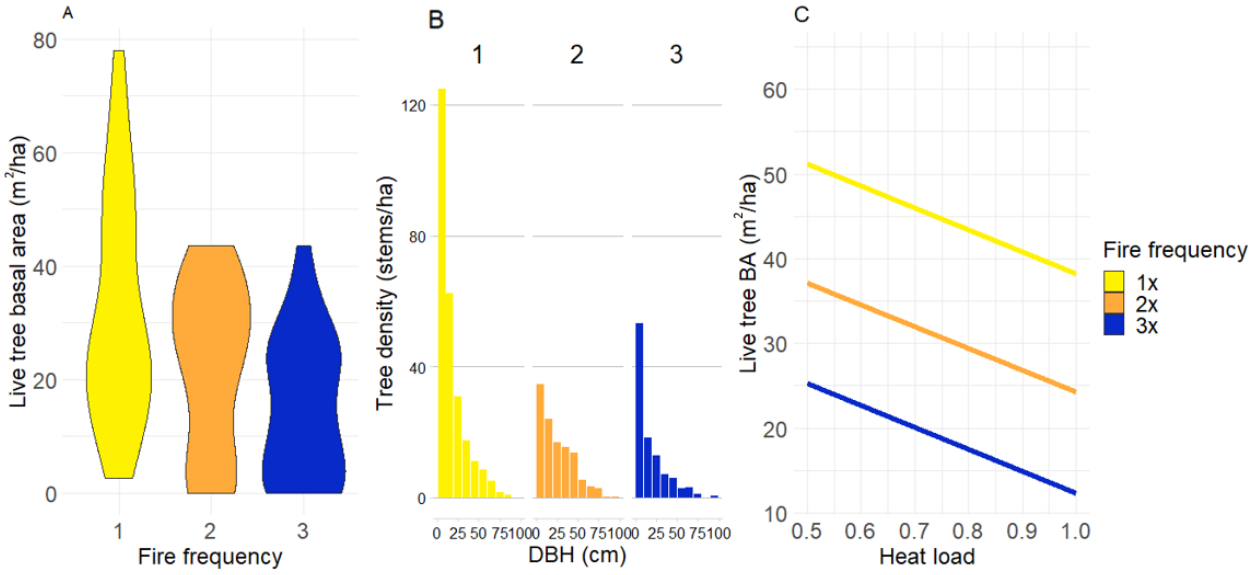

Figure 3. Live tree structure variables. (A) Basal area of live trees by number of times burned. (B) Distribution of diameter at breast height (DBH) classes by trees per hectare in 10 cm bins. (C) Predicted values of live tree basal area across heat load. Heat load is an unitless index scaled to the solar radiation that a site receives, and is calculated from latitude, aspect, and slope; it accounts for south-west facing slopes being warmer (higher heat load values) than north-east facing slopes (lower heat load values) (McCune and Keon 2002)

Tree regeneration was abundant across all three burn histories. Regeneration was not limited by seed source availability as 99% of plots (all but one) were within 200 m of a conifer seed source. The average distance to seed source for once-burned, twice-burned, and thrice-burned sites was 2.6 m, 11.9 m, and 28.1 m, respectively. The increasing distance to seed source did not negatively impact seedling recruitment (Figure 4). Saplings, 1.37 m in height up to 10 cm in DBH, are included in the DBH distribution figure (Figure 3b). Mean sapling density was

highest in the thrice-burned sites (200 stems/ha), followed by twice-burned (176 stems/ha), and once-burned (144 stems/ha).

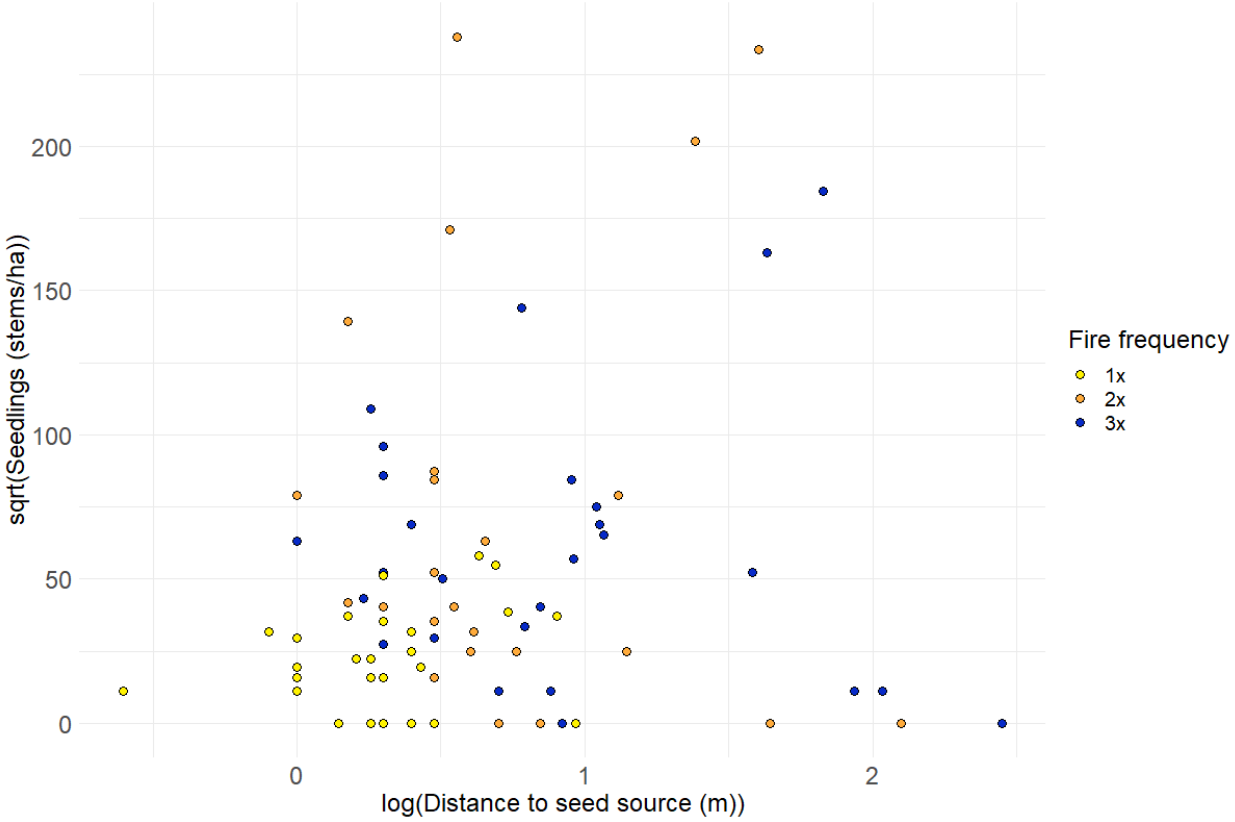

Figure 4. Distribution of seedlings based on seed source proximity. Log base 10.

There were more seedlings in the twice- and thrice-burned sites compared to the once-burned sites (Figure 5a) with mean seedling density for once-, twice-, and thrice-burned of 943 stems/ha, 10,293 stems/ha, and 6,903 stems/ha, respectively. Seedlings species found within the study area included *Abies grandis, Pseudotsuga menziesii, Picea engelmannii, Pinus ponderosa, Thuja plicata*, though most were *Abies grandis* and *Pseudotsuga menziesii*. *Abies grandis* was the most abundant species of tree regeneration across all three fire frequencies but was proportionally higher in the once-burned sites, while *Pseudotsuga menziesii* was proportionally higher in the twice- and thrice-burned sites. *Abies grandis* had a mean of 1,952 stems/ha in the

once-burned area and had mean 15,292 stems/ha and mean 9,088 stems/ha in twice- and thrice-burned area, respectively (Figure 5b). *Pseudotsuga menziesii* had even less seedlings in the once-burned with a mean of 625 stems/ha with a larger contrast to the twice- and thrice-burned with a mean of 10,542 stems/ha and a mean of 6,184 stems/ha, respectively (Figure 5c).

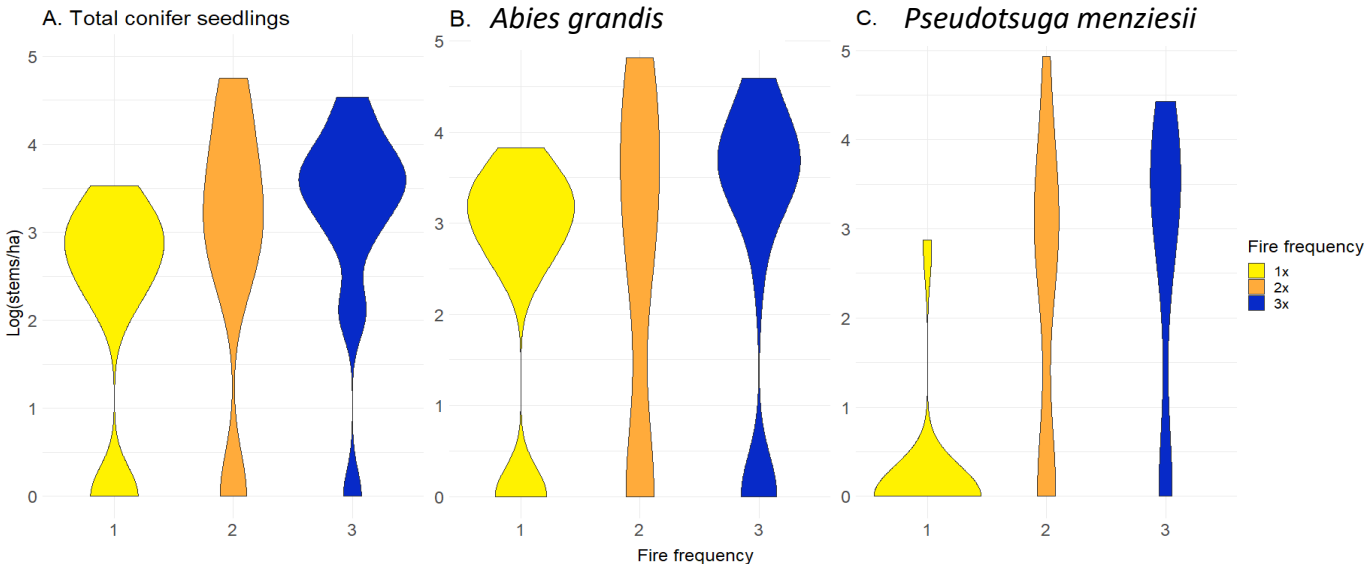

Figure 5. Conifer tree regeneration by fire frequency. (A) Abundance of all seedlings of all species by burn frequency. (B) Abundance of *Abies grandis* seedlings by fire frequency. (C) Abundance of *Pseudotsuga menziesii* seedlings by fire frequency

Standing dead trees and down woody material

Standing dead tree basal area increased (P = 0.003) with increasing fire frequency (Figure 6A; Figure 6B; Table 2). Dead basal area was inversely related to heat load (0.078, Table 2), with high heat load sites (more southwesterly slopes with higher radiation loads) having lower dead basal area within fire frequency classes (Figure 6B). Once-burned sites had a mean dead basal area of 3.8 m^2/ha while twice- and thrice-burned had a mean basal area of 14.0 m^2/ha and 15.0 m^2/ha, respectively. Dead basal area increased (P = 0.009) with increasing TWI (Table 2).

Table 2. ANOVA tables √Dead Basal area GLMM with the important explanatory variables and their associated F- and p-values. The sign in the variable category denotes the sign of the coefficient.

Variable	F-value	p-value
Fire frequency (+)	8.30	0.003
TWI (+)	7.27	0.009
Heat load (-)	3.23	0.078

CWM increased (P = 0.08) with increasing fire frequency (Figure 6C and 6D, Table 3). CWM was inversely related to heat load (P = 0.01, Table 3), with high heat load sites (more southwesterly slopes with high radiation loads) having less CWM within fire frequency classes (Figure 6D). The mean fuel load for CWM for once-, twice-, and thrice-burned sites was 184 m^3/ha, 303 m^3/ha, and 306 m^3/ha, respectively. CWM had a weak positive relationship with TWI (Table 3; Table A6). As seen in Figure 6D, the predicted lines for twice- and thrice-burned are very similar and there is a large departure from the once-burned predicted values.

Table 3. ANOVA table √CWM GLMM with the important explanatory variables and their associated F- and p-values. The sign in the variable category denotes the sign of the coefficient.

Variable	F-value	p-value
Fire frequency (+)	3.01	0.08
TWI (+)	3.65	0.06
Heat load (-)	6.70	0.01

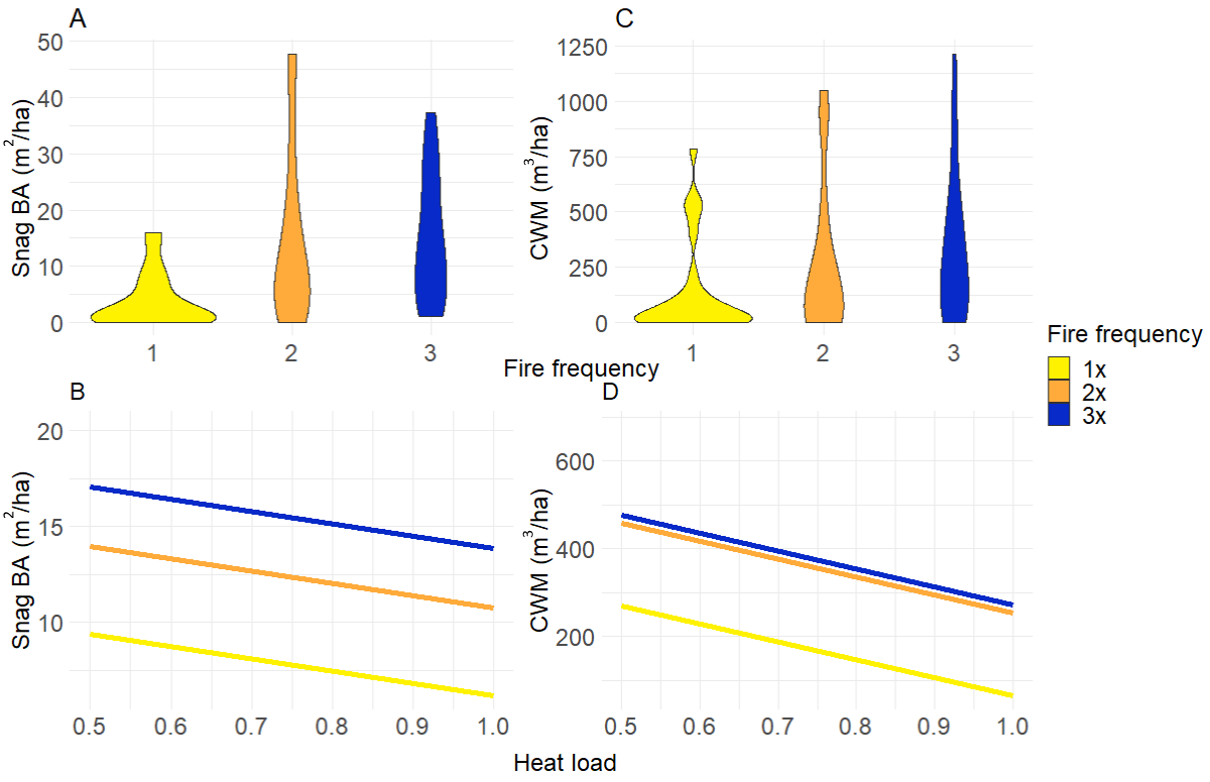

Figure 6. Dead woody material variables. (A) Volume of coarse woody material (CWM) by fire frequency. (B) Predicted values of CWM across heat load. (C) Basal area of snags by fire frequency. (D) Predicted values of snag basal area across heat load.

Other fuels variables measured include 1-, 10-, and 100-hour fuels as well as litter and duff (Table B2). One-hour fuels were very similar across all three burn histories but skewed higher slightly for the once-burned (median 0.06 kg/m^2) compared to twice- (median 0.05 kg/m^2) and thrice-burned (median 0.05 kg/m^2) sites. Ten-hour fuels had the highest mean (0.11 kg/m^2) but the lowest median (0.04 kg/m^2) in the once-burned compared to the twice-burned (mean 0.08 kg/m^2, median 0.05 kg/m^2) and thrice-burned (mean 0.09 kg/m^2, median 0.06 kg/m^2). Hundred-hour fuel loadings were highest in the twice-burned (mean 0.18 kg/m^2) followed by the thrice-burned (0.14 kg/m^2) and once-burned (0.12 kg/m^2). Both litter and duff depths were inversely related to fire frequency.

Live fuels: shrubs and herbs

Shrub load was not related (P = 0.50) to fire history (Table 4; Figure 7) or TWI (P = 0.99), and marginally related to heat load (P = 0.11). Mean shrub load for once-, twice-, and thrice-burned sites was 0.46 kg/m^2, 0.24 kg/m^2, and 0.39 kg/m^2 (Figure 7A), respectively. Herb load was not related to fire frequency (P = 0.84) and had a mean of 0.04 kg/m^2 for all burn histories (Table 5; Figure 7B). Heat load (P = 0.61) and TWI (P = 0.32) were also not related to herb load.

Table 4. ANOVA tables √Shrubs GLMM with the important explanatory variables and their associated F- and p-values. The sign in the variable category denotes the sign of the coefficients.

Variable	F-value	p-value
Fire frequency	0.73	0.50
TWI	0.0001	0.99
Heat load (+)	2.69	0.11

Table 5. ANOVA tables √Herbs GLMM with the important explanatory variables and their associated F- and p-values. The sign in the variable category denotes the sign of the coefficient.

Variable	F-value	p-value
Fire frequency	0.18	0.84
TWI	1.01	0.32
Heat load	0.26	0.61

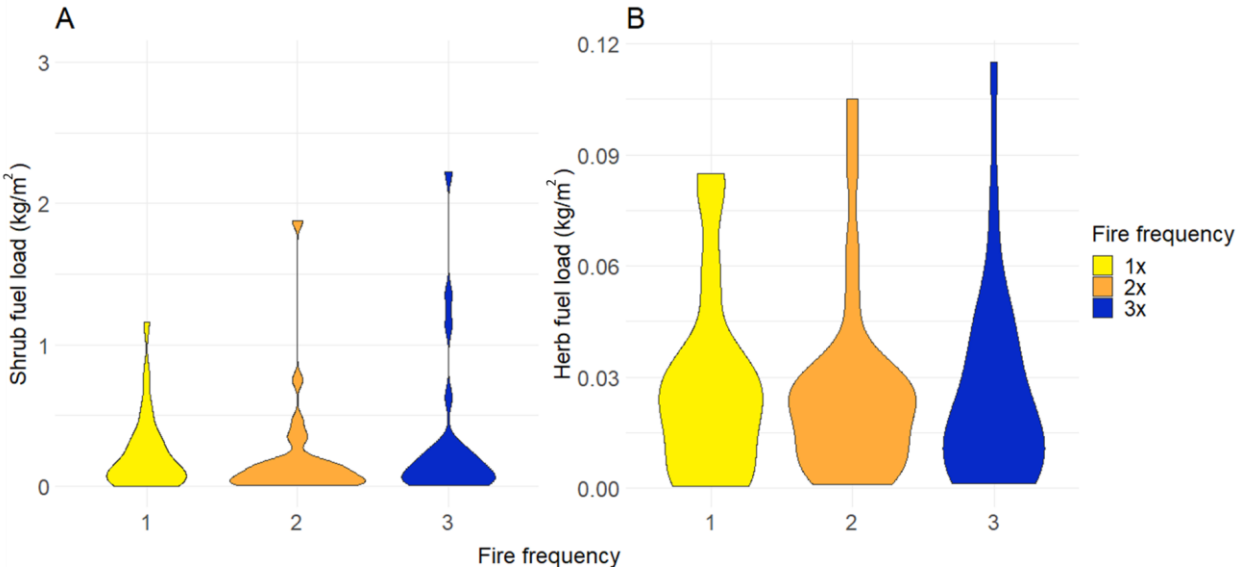

Figure 7. Live fuels across fire frequency (A) Shrub load by fire frequency (B) Herb load by fire frequency.

Shrub dominated sites were characterized by high heat load and low overstory tree basal area, independent of fire history. High shrub loads only occurred at sites where both heat load was >0.65 and live tree basal area was <30 m^2/ha (Figure 8A). Herb load had a similar but less drastic pattern. Herbs were more abundant on sites with high heat load (>0.6) and low live overstory tree basal area (<40 m^2/ha) (Figure 8B).

Quantile regression showed some support for these patterns. Both regression coefficients for heat load and BA became more extreme the higher the percentile of data they were modeling. The 0.25 quantile had a significant live tree BA with a p-value of 0.05 though heat load was insignificant with a p-value of 0.949. The lowest p-value of heat load for shrubs was 0.152 at the 0.75 quantile with an estimate of 0.280. The corresponding live tree BA had a p-value of 0.264 with an estimate of -0.003. For herbs, heat load was insignificant on all quantiles, with the lowest

p-value of 0.70 at 0.25 quantile. Live tree BA was more important, it had a p-value of 0.08 at 0.75 quantile and an estimate of -0.0003.

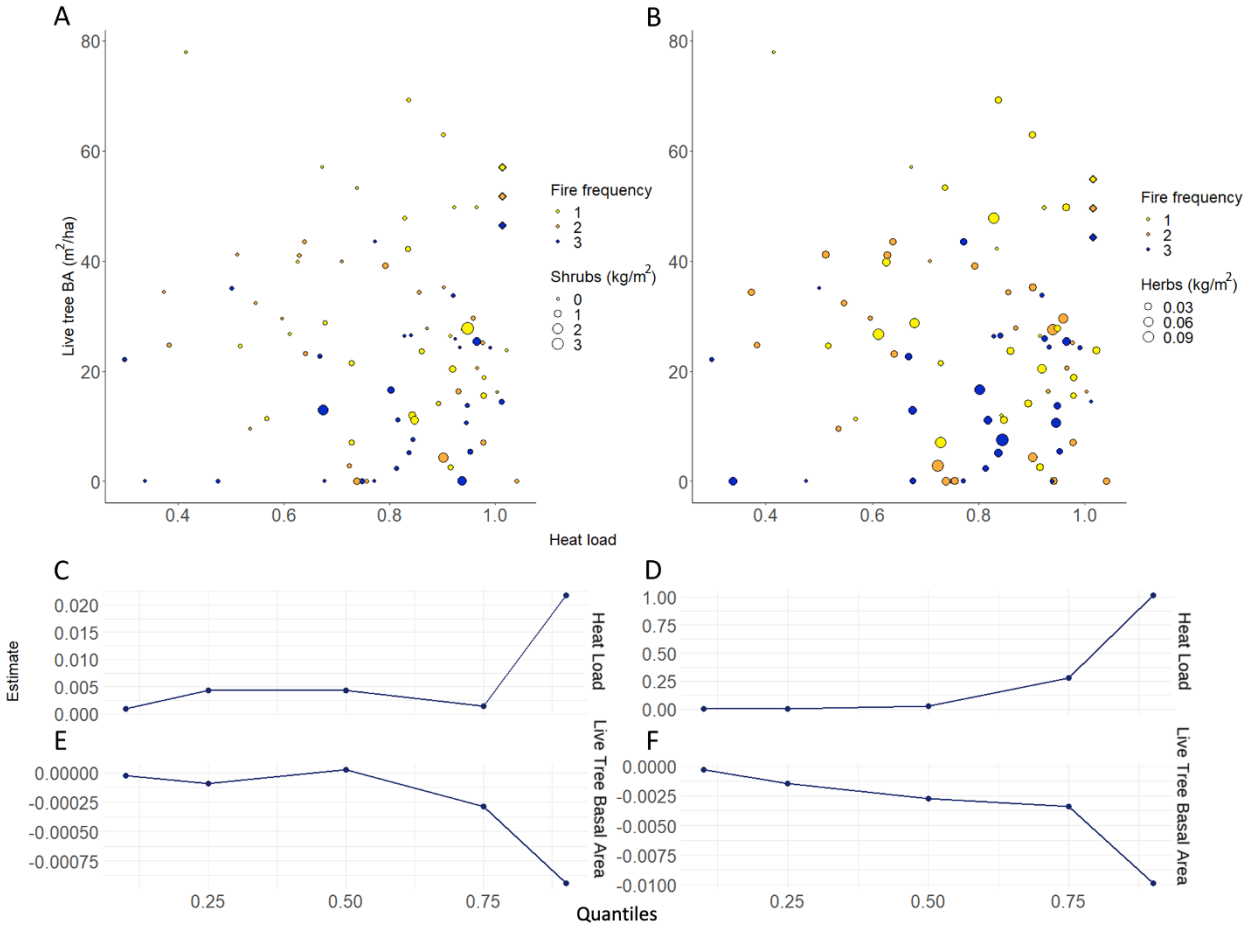

Figure 8. (A) Variation of shrub biomass across live tree basal area (BA) and heat load. (B) Variation of herb biomass across live tree BA and heat load. (C) Quantile regression of shrubs by heat load where Tau is the different quantiles. (D) Quantile regression of herbs by heat load. (E) Quantile regression of shrubs by live tree BA. (F) Quantile regression of herbs by live tree BA.

Forest structure, composition, and fuels in PCA space

Differences of forest structure, composition, and fuels (Figure B1) among fire frequencies were evident in the PCA visualizations (Figure 9). The first three axes of the PCA explained 20.6%, 16.7%, 11.5% of variation in the data, respectively (Figure 9). The first axis represents fire resistance or sensitivity to burn history, from low (left) to high (right). Fire history showed the greatest separation across axis one, with the once-burned sites occupying the left end of the gradient and the twice- and thrice-burned sites shifted to the right on axis one. The second axis represents life form dominance, where low or negative values correspond to shrub and herb dominated areas and high or positive values represent more tree dominated areas. The third axis represents canopy cover gradient, where the positive values represent more open canopy attributes, and the negative values represent more closed canopy attributes. There is little separation of burn history across axes two and three. This is consistent with the analysis of shrub and herb fuel loading in relation to fire history (Figure 7), where these variables were not related to fire history. The highest correlation of coefficients was seedlings per hectare and dead BA at 0.65. The next highest correlation of two variables was canopy cover and live tree basal area at 0.62 (Figure B2).

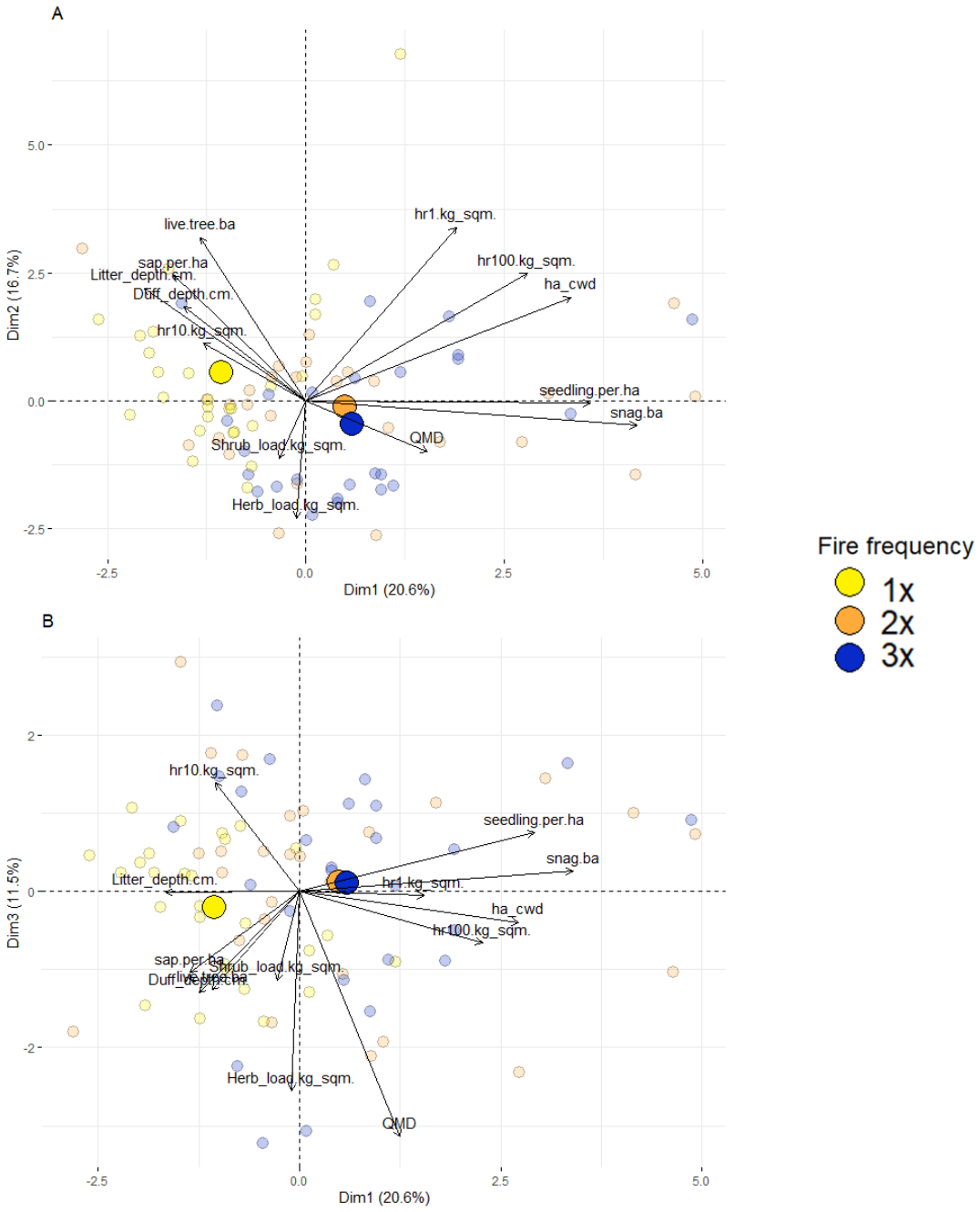

Figure 9. Principal Component Analysis of forest structure and fuels variables for each fire frequency. The first three principal components explain 48.8% of the total variability in the dataset. Dimension one represents fire resistance or sensitivity to burn history. Dimension two represents life form dominance. Dimension three represents a canopy cover gradient.

Discussion

My findings include the differences in key ecological variables and quantify the effect that an initial high-severity fire followed by different subsequent fire histories has on fuels, forest structure and composition, and tree regeneration. My results highlight the distinct forest communities that exist in the SBW and help quantify how fire frequency over the past century shapes forest composition and fire hazard and fuel loading on the contemporary landscape. Higher fire frequency was associated with lower live tree basal area and higher snag basal area and CWM biomass. Topographic variables affected these structure variables, with a consistent effect of reduced live and dead tree structure on high heatload (more southwesterly) sites.

Forest composition reflects fire frequency

Fire frequency affects composition and abundance of both mature trees and seedlings. Fire tends to kill smaller trees because they have less developed fire-resistance traits than more mature trees (i.e., thinner bark and lower crowns) of the same species. This pattern was exacerbated by the species composition of the area, especially the high percentage of *Abies grandis* in these forests, which tend to not be very fire-resistant (Stevens et al. 2020). This variability in space was found in the results as fire frequency increased live tree QMD and decreased density. With increasing fire frequency, the percent composition of *Abies grandis* decreased (Larson et al. 2013, Belote et al. 2015). This is especially evident in the contrast between the once-burned photo example (Figure 10B) and the thrice-burned photo example (Figure 10F) where the once-burned example has small trees and saplings, and the thrice-burned example has only widely spaced large trees.

Recently burned (i.e., 2x and 3x fire frequency) sites had more tree regeneration than sites that burned only once due to landscape composition and forest type. There was no lack of

seed source due to the heterogeneity of the burns and the mosaic of fires and subsequent forest age across the landscape (McDonald 1980). Though many recent regeneration studies have found alarming patterns of regeneration failure in western US conifer forests (Stevens-Rumann et al. 2018, Davis et al. 2019), this was not the case with my findings. Though many of these studies occurred in subalpine or low elevation drier ecotones which may be more susceptible to regeneration failure. However, in the wetter environment of the SBW, trees are regenerating across all fire histories, similar to findings from other moist-mixed conifer forests (Povak et al. 2020). Seed source was not a limiting factor for any burn history. This might be because there was no logging, leaving larger trees that are more likely to survive fire and provide seeds (Larson et al. 2013). The lack of limited seed source I found is in contrast to other studies (Kemp et al. 2016, Harvey et al. 2016, Coop et al. 2020b). This may be because the high-severity patches within the SBW are in a less constrained fire regime with less suppression.

Pseudotsuga menziesii was more abundant in reburns and thus was acting as more of an early seral species; having more successful regeneration in twice- and thrice-burned sites with more open canopy, and less litter and duff. *Abies grandis* was more abundant (in relative terms) in the once-burned sites that had fire less recently. This species was able to regenerate in more closed canopy areas with higher litter and duff levels; thus, acting as a later seral species. True shade-intolerant species regeneration (*Pinus ponderosa, Pinus contorta,* and *Larix occidentalis*) was rare. This is consistent with the rarity of these species in the overstory—there is limited seed source for these species across the study area. Even with an active fire regime, with a lack of local seed source, these shade-intolerant species cannot regenerate. In similar mesic *Abies grandis* and *Pseudotsuga menziesii* forests outside the wilderness, post-fire planting of such

species may be required to increase representation of these species on the landscape, if that is a management goal.

Fire history impacts fuels for decades

Both standing dead trees and CWM were lowest in the once-burned sites and increased with increasing fire frequency. However, CWM was more impacted by time since fire, rather than fire frequency. That is, CWM values for twice- and thrice-burned were similarly higher than the once-burned sites. Standing dead trees and CWM ultimately originate the same source—live trees—but have different pathways and residence times to reach their status. Live trees become snags, then snags tops break or rot topples them and they become CWM (Harmon et al. 1986, Franklin et al. 1987, Stevens-Rumann et al. 2020). Fires also accelerate transition of standing snags to CWM material when fires burn through snag bases, causing snags to fall (Cansler et al. 2019). Conversion of snags to CWM is also impacted by site condition (Stevens-Rumann et al. 2020); which may be why heat load and TWI were important explanatory variables for standing dead wood and CWM. The differences between the twice- and thrice- burned sites for these fuels is caused by reburns both consuming dead wood and increasing the pool of dead woody through fire-caused mortality (Donato et al. 2016). CWM has a longer residence time than snags and has two potential fates: with fire immediate consumption in reburns (Figure 10E & F), or without fire a slow decomposition (Figure 10B) (Ward et al. 2017).

Woody fine fuels had lots of variation, typical of these variables (Keane 2015). One-hour, 10-hour, and 100-hour fuels differed little across burn histories; this is due to the landscape sampling occurring in relatively tree-dominated areas and fine fuels being both ephemeral and mobile. They may originate from either live or dead wood and thus the supply is high compared to the losses. Ground fuels have an inverse relationship with fire frequency, which may be

related to time since fire. Litter and duff take time to accumulate and have high consumption rates in most fires regardless of severity (Cansler et al. 2019, Larson et al. 2020, Stevens-Rumann et al. 2020).

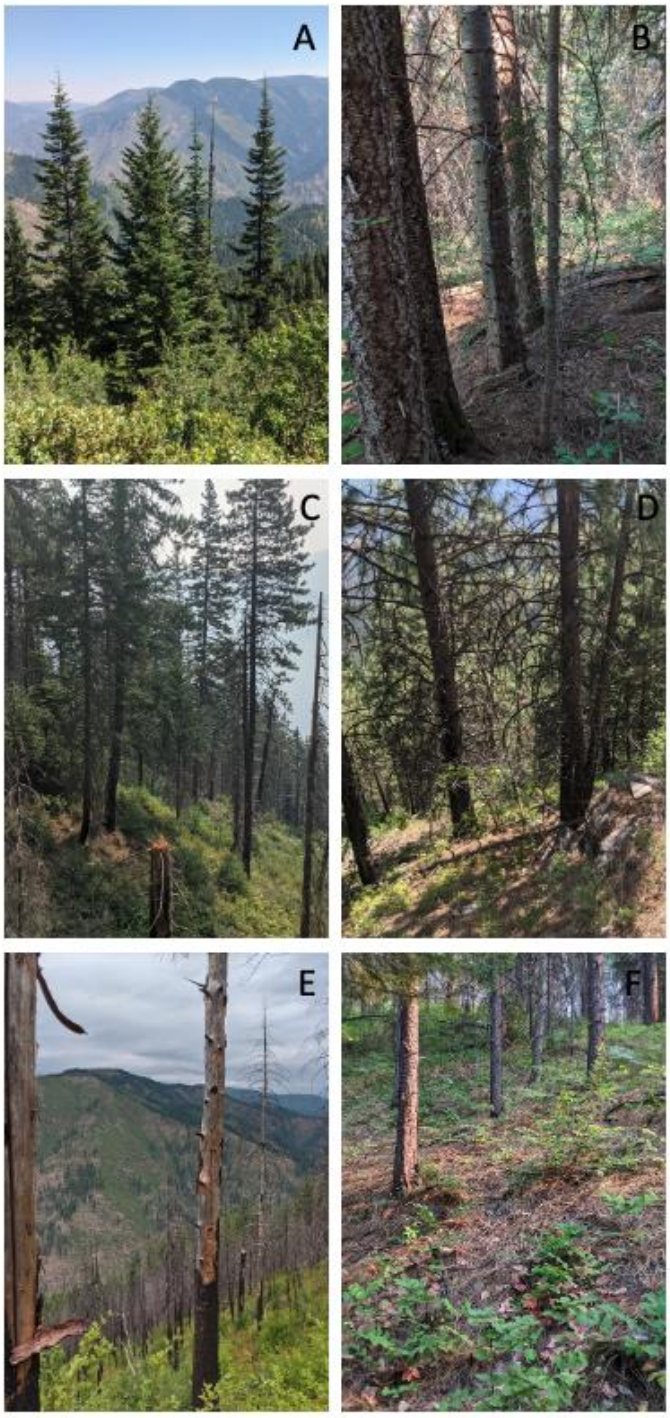

Figure 10. Photos illustrating representative conditions from select sample plots. (A & B) once-burned, (C&D) twice-burned, (E&F) thrice-burned. Northern Rocky Mountain Mesic Montane Mixed Conifer Forest (LANDFIRE 2016), Selway-Bitterroot Wilderness, Idaho, USA.

Live fuels: shrubs and herbs

Neither shrubs nor herbs were significantly related to fire frequency. This is evident in the photo examples of all three fire histories having substantial amount of fuels present (Figure 10). Environmental interactions were expressed in the quartile regression. Where there was higher basal area, there were less shrubs, suggesting a competitive effect of overstory trees on the growth and biomass accumulation of shrubs in the understory (Tepley et al. 2018, Jaffe et al. 2021).

Hotter and drier sites, with higher heat load, are more likely to have converted from forest to shrublands following the initial high-severity fire in the early 20th century (Figure 7) (Coop et al. 2020). This type change to shrubs can remain in this alternative stable state as shrubs can sometimes sustain more frequent burning (Ferguson and Byrne 2016, Coop et al. 2020). Trees were either unable to establish or there were very spare mature trees interspersed with mature shrubs. This suggests that shrubs were more competitive in this environment (Donato et al. 2016, Stevens-Rumann and Morgan 2016, Harvey et al. 2016). However, this pathway was rare in our dataset—most sites have regenerated to tree-dominated forest communities.

Conclusion and Management Implications

Fire creates a lasting effect on the landscape because it affects tree regeneration as well as forest structure and fuels. Understanding the present condition of areas that have been burned at high severity in the past may help us understand what present high-severity burns might look like in the future. A few areas (4%) in this study have not regenerated back to forests; most have. They are populated with mature trees and have conifer regeneration. The large amount of fire that has occurred within the SBW has led to a heterogeneous landscape mosaic with a high

degree of structural variability (Figure 10), illustrating how active mixed-severity fire regimes create and maintain ecological complexity.

Wilderness serves as a great natural laboratory for fire and ecosystem science, particularly wilderness areas with less suppression (Seielstad 2015, Kreider et al. 2022). This study could not have been conducted outside of a wilderness area as the pattern and process of fire was essential to this study and wilderness areas have the most intact fire regimes. Wilderness was also a requirement because of the need for unharvested sites allowed to develop for a century after initial high-severity fire.

Th results of this study may be used to inform silvicultural practices for mesic forests in the Northern Rockies. It shows the success of natural regeneration, even with multiple disturbances. Though even in this natural fire regime, there is limited overstory and regeneration of shade-intolerant species. If there is an objective to have more of those species, planting may need to occur in non-wilderness settings. This study also shows that mixed-severity fire regime leads to wide variability in forest structure, which is helpful for retention harvest practices trying to mimic natural processes.

Acknowledgments

I recognize that the study area includes the unceded ancestral lands of the Nez Perce (Nimiipuu), Salish (Séliš) Kootenai, Shoshone-Bannock, and Lemhi-Shoshone peoples. I thank the Selway-Bitterroot Wilderness managers for making this study possible through their support and resources. I would also like to thank Pat Greene for creating and allowing me to use her geospatial dataset. I greatly appreciate Carmen Murrill, William DeGrandpre, and Mich Clarkson for assisting with field data collection. I thank Mark Krieder for assisting with field work and also for supporting and mentoring me through geospatial analysis. I am grateful for Dr. Dave Affleck for his assistance and mentorship with setting up sampling design and analysis of models. I would like to thank my committee members, Drs. Sean Parks, Carl Seielstad, and Phil Higuera, for their advice, guidance, and support, especially my major advisor, Dr. Andrew Larson.

Literature Cited

Abatzoglou, J. T., C. A. Kolden, A. P. Williams, J. A. Lutz, and A. M. S. Smith. 2017. Climatic influences on interannual variability in regional burn severity across western US forests. International Journal of Wildland Fire 26:269–275.

Abatzoglou, J. T., and A. P. Williams. 2016a. Impact of anthropogenic climate change on wildfire across western US forests. Proceedings of the National Academy of Sciences 113:11770–11775.

Abatzoglou, J. T., and A. P. Williams. 2016b. Impact of anthropogenic climate change on wildfire across western US forests. Proceedings of the National Academy of Sciences 113:11770.

Belote, R.T., A. J. Larson, and M. S. Dietz. 2015. Tree survival scales to community-level effects following mixed-severity fire in a mixed-conifer forest. Forest Ecology and Management 353:221–231.

Berkey, J. K., R. T. Belote, C. T. Maher, and A. J. Larson. 2021. Structural diversity and development in active fire regime mixed-conifer forests. Forest Ecology and Management 479:118548.

Beven, K. J., and M. J. Kirkby. 1979. A physically based, variable contributing area model of basin hydrology / Un modèle à base physique de zone d'appel variable de l'hydrologie du bassin versant. Hydrological Sciences Bulletin 24:43–69.

Brenning, A., D. Bangs, and M. Becker. 2018. RSAGA: SAGA Geoprocessing and Terrain Analysis.

Brunelle, A., C. Whitlock, P. Bartlein, and K. Kipfmueller. 2005. Holocene fire and vegetation along environmental gradients in the Northern Rocky Mountains. Quaternary Science Reviews 24:2281–2300.

Busby, S. U., K. B. Moffett, and A. Holz. 2020. High-severity and short-interval wildfires limit forest recovery in the Central Cascade Range. Ecosphere 11:e03247.

Cansler, C. A., M. E. Swanson, T. J. Furniss, A. J. Larson, and J. A. Lutz. 2019. Fuel dynamics after reintroduced fire in an old-growth Sierra Nevada mixed-conifer forest. Fire Ecology 15:16.

Coop, J. D., S. A. Parks, C. S. Stevens-Rumann, S. D. Crausbay, P. E. Higuera, M. D. Hurteau, A. Tepley, E. Whitman, T. Assal, B. M. Collins, K. T. Davis, S. Dobrowski, D. A. Falk, P. J. Fornwalt, P. Z. Fulé, B. J. Harvey, V. R. Kane, C. E. Littlefield, E. Q. Margolis, M. North, M.-A. Parisien, S. Prichard, and K. C. Rodman. 2020a. Wildfire-Driven Forest Conversion in Western North American Landscapes. BioScience 70:659–673.

Coop, J. D., S. A. Parks, C. S. Stevens-Rumann, S. D. Crausbay, P. E. Higuera, M. D. Hurteau, A. Tepley, E. Whitman, T. Assal, B. M. Collins, K. T. Davis, S. Dobrowski, D. A. Falk, P. J. Fornwalt, P. Z. Fulé, B. J. Harvey, V. R. Kane, C. E. Littlefield, E. Q. Margolis, M. North, M.-A. Parisien, S. Prichard, and K. C. Rodman. 2020b. Wildfire-Driven Forest Conversion in Western North American Landscapes. BioScience 70:659–673.

Davis, K. T., S. Z. Dobrowski, P. E. Higuera, Z. A. Holden, T. T. Veblen, M. T. Rother, S. A. Parks, A. Sala, and M. P. Maneta. 2019. Wildfires and climate change push low-elevation forests across a critical climate threshold for tree regeneration. Proceedings of the National Academy of Sciences 116:6193–6198.

Davis, K. T., P. E. Higuera, S. Z. Dobrowski, S. A. Parks, J. T. Abatzoglou, M. T. Rother, and T. T. Veblen. 2020. Fire-catalyzed vegetation shifts in ponderosa pine and Douglas-fir forests of the western United States. Environmental Research Letters 15:1040b8.

Donato, D. C., J. B. Fontaine, and J. L. Campbell. 2016. Burning the legacy? Influence of wildfire reburn on dead wood dynamics in a temperate conifer forest. Ecosphere 7:e01341.

Eilers, P. H. C., and B. D. Marx. 1996. Flexible smoothing with B-splines and penalties. Statistical Science 11:89–121.

Ferguson, D. E., and J. C. Byrne. 2016. Shrub succession on eight mixed-severity wildfires in western Montana, northeastern Oregon, and northern Idaho. Page RMRS-RP-106. U.S. Department of Agriculture, Forest Service, Rocky Mountain Research Station, Ft. Collins, CO.

Filho, A. F., S. A. Machado, and M. R. A. Carneiro. 2000. Testing accuracy of log volume calculation procedures against water displacement techniques (xylometer) 30:8.

Finklin, A. I. 1983. Weather and climate of the Selway-Bitterroot Wilderness. University of Idaho Press, Moscow, Idaho, USA.

Franklin, J. F., H. H. Shugart, and M. E. Harmon. 1987. Tree Death as an Ecological Process. BioScience 37:550–556.

Harmon, M. E., J. F. Franklin, F. J. Swanson, P. Sollins, S. V. Gregory, J. D. Lattin, N. H. Anderson, S. P. Cline, N. G. Aumen, J. R. Sedell, G. W. Lienkaemper, K. Cromack, and K. W. Cummins. 1986. Ecology of Coarse Woody Debris in Temperate Ecosystems. Pages 133–302 *in* A. MacFadyen and E. D. Ford, editors. Advances in Ecological Research. Academic Press.

Harvey, B. J., D. C. Donato, and M. G. Turner. 2016. Drivers and trends in landscape patterns of stand-replacing fire in forests of the US Northern Rocky Mountains (1984–2010). Landscape Ecology 31:2367–2383.

Hessburg, P. F., D. J. Churchill, A. J. Larson, R. D. Haugo, C. Miller, T. A. Spies, M. P. North, N. A. Povak, R. T. Belote, P. H. Singleton, W. L. Gaines, R. E. Keane, G. H. Aplet, S. L. Stephens, P. Morgan, P. A. Bisson, B. E. Rieman, R. B. Salter, and G. H. Reeves. 2015. Restoring fire-prone Inland Pacific landscapes: seven core principles. Landscape Ecology 30:1805–1835.

Hessburg, P. F., S. J. Prichard, R. K. Hagmann, N. A. Povak, and F. K. Lake. 2021. Wildfire and climate change adaptation of western North American forests: a case for intentional management. Ecological Applications 31:e02432.

Heyerdahl, E. K., L. B. Brubaker, and J. K. Agee. 2001. Spatial Controls of Historical Fire Regimes: A Multiscale Example from the Interior West, USA. Ecology 82:660–678.

Hoecker, T. J., and M. G. Turner. 2022. A short-interval reburn catalyzes departures from historical structure and composition in a mesic mixed-conifer forest. Forest Ecology and Management 504:119814.

Huff, M. H. 1995. Forest Age Structure and Development Following Wildfires in the Western Olympic Mountains, Washington. Ecological Applications 5:471–483.

Jaffe, M. R., B. M. Collins, J. Levine, H. Northrop, F. Malandra, D. Krofcheck, M. D. Hurteau, S. L. Stephens, and M. North. 2021. Prescribed fire shrub consumption in a Sierra Nevada mixed-conifer forest. Canadian Journal of Forest Research 51:1718–1725.

Keane, R. E. 2015. Wildland Fuel Fundamentals and Applications. Springer International Publishing, Cham.

Keane, R. E., and L. J. Dickinson. 2007. The photoload sampling technique: estimating surface fuel loadings from downward-looking photographs of synthetic fuelbeds. Page RMRS-

GTR-190. U.S. Department of Agriculture, Forest Service, Rocky Mountain Research Station, Ft. Collins, CO.

Kemp, K. B., P. E. Higuera, and P. Morgan. 2016. Fire legacies impact conifer regeneration across environmental gradients in the U.S. northern Rockies. Landscape Ecology 31:619–636.

Key, C. H., and N. C. Benson. 2006. Landscape Assessment (LA):55.

Kipfmueller, K. F., and J. A. Kupfer. 2005. Complexity of Successional Pathways in Subalpine Forests of the Selway-Bitterroot Wilderness Area. Annals of the Association of American Geographers 95:495–510.

Koenker, R. 2021. quantreg: Quantile Regression.

LANDFIRE. 2016. Existing Vegetation Type (EVT) CONUS. U.S. Department of the Interior, Geological Survey, and U.S. Department of Agriculture.

Larsen, J. A. 1925. Natural reproduction after forest fires in northern Idaho. Journal of Agricultural Research 12:1177–1197.

Larson, A. J., R. T. Belote, C. A. Cansler, S. A. Parks, and M. S. Dietz. 2013. Latent resilience in ponderosa pine forest: effects of resumed frequent fire. Ecological Applications 23:1243–1249.

Larson, A. J., J. K. Berkey, C. T. Maher, W. Trull, R. T. Belote, and C. Miller. 2020. Fire history (1889-2017) in the South Fork Flathead River Watershed within the Bob Marshall Wilderness (Montana), including effects of single and repeat wildfires on forest structure and fuels. In: Hood, Sharon M.; Drury, Stacy; Steelman, Toddi; Steffens, Ron,[eds.]. Proceedings of the Fire Continuum-Preparing for the future of wildland fire; 2018 May

21-24; Missoula, MT. Proceedings RMRS-P-78. Fort Collins, CO: US Department of Agriculture, Forest Service, Rocky Mountain Research Station. p. 139-156. 78:139–156.

Larson, A. J., J. A. Lutz, R. F. Gersonde, J. F. Franklin, and F. F. Hietpas. 2008. Potential Site Productivity Influences the Rate of Forest Structural Development. Ecological Applications 18:899–910.

Littell, J. S., D. McKenzie, H. Y. Wan, and S. A. Cushman. 2018. Climate Change and Future Wildfire in the Western United States: An Ecological Approach to Nonstationarity. Earth's Future 6:1097–1111.

Lutes, D. C., R. E. Keane, J. F. Caratti, C. H. Key, N. C. Benson, S. Sutherland, and L. J. Gangi. 2006. FIREMON: Fire effects monitoring and inventory system. Page RMRS-GTR-164. U.S. Department of Agriculture, Forest Service, Rocky Mountain Research Station, Ft. Collins, CO.

McCune, B., and D. Keon. 2002. Equations for potential annual direct incident radiation and heat load. Journal of Vegetation Science 13:603–606.

McDonald, P. M. 1980. Seed Dissemination in Small Clearcuttings in North-central California. U.S. Department of Agriculture, Forest Service, Pacific Southwest Forest and Range Experiment Station.

Meigs, G. W., C. J. Dunn, S. A. Parks, and M. A. Krawchuk. 2020. Influence of topography and fuels on fire refugia probability under varying fire weather conditions in forests of the Pacific Northwest, USA. Canadian Journal of Forest Research 50:636–647.

Morgan, P., E. K. Heyerdahl, and C. E. Gibson. 2008. Multi-season climate synchronized forest fires throughout the 20th century, Northern Rockies, USA. Ecology 89:717–728.

Morgan, P., E. K. Heyerdahl, C. Miller, A. M. Wilson, and C. E. Gibson. 2014. Northern Rockies Pyrogeography: an Example of Fire Atlas Utility. Fire Ecology 10:14–30.

Parks, S. A., and J. T. Abatzoglou. 2020a. Warmer and Drier Fire Seasons Contribute to Increases in Area Burned at High Severity in Western US Forests From 1985 to 2017. Geophysical Research Letters 47:e2020GL089858.

Parks, S. A., and J. T. Abatzoglou. 2020b. Warmer and Drier Fire Seasons Contribute to Increases in Area Burned at High Severity in Western US Forests From 1985 to 2017. Geophysical Research Letters 47:e2020GL089858.

Parks, S. A., L. M. Holsinger, M. J. Koontz, L. Collins, E. Whitman, M.-A. Parisien, R. A. Loehman, J. L. Barnes, J.-F. Bourdon, J. Boucher, Y. Boucher, A. C. Caprio, A. Collingwood, R. J. Hall, J. Park, L. B. Saperstein, C. Smetanka, R. J. Smith, and N. Soverel. 2019. Giving Ecological Meaning to Satellite-Derived Fire Severity Metrics across North American Forests. Remote Sensing 11:1735.

Parks, S. A., L. M. Holsinger, C. Miller, and C. R. Nelson. 2015a. Wildland fire as a self-regulating mechanism: the role of previous burns and weather in limiting fire progression. Ecological Applications 25:1478–1492.

Parks, S. A., L. M. Holsinger, C. Miller, and C. R. Nelson. 2015b. Fire atlas for the Selway-Bitterroot Wilderness. Forest Service Research Data Archive.

Parks, S. A., C. Miller, C. R. Nelson, and Z. A. Holden. 2014. Previous Fires Moderate Burn Severity of Subsequent Wildland Fires in Two Large Western US Wilderness Areas. Ecosystems 17:29–42.

Parks, S. A., M.-A. Parisien, C. Miller, L. M. Holsinger, and L. S. Baggett. 2018. Fine-scale spatial climate variation and drought mediate the likelihood of reburning. Ecological Applications 28:573–586.

Pinheiro, J., D. Bates, and S. DebRoy. 2022. {nlme}: Linear and Nonlinear Mixed Effects Models.

Povak, N.A., D.J. Churchill, C.A. Cansler, P.F. Hessburg, V.R. Kane, J.T. Kane, J.A. Lutz, A.J. Larson. 2020. Wildfire severity and postfire salvage harvest effects on long-term forest regeneration. Ecosphere 11(8): e03199.

Prichard, S. J., C. S. Stevens-Rumann, and P. F. Hessburg. 2017. Tamm Review: Shifting global fire regimes: Lessons from reburns and research needs. Forest Ecology and Management 396:217–233.

Rollins, M., T. Swetnam, and P. Morgan. 2000. Twentieth-century fire patterns in the Selway-Bitterroot Wilderness Area, Idaho/Montana, and the Gila/Aldo Leopold Wilderness Complex, New Mexico. In: Cole, David N.; McCool, Stephen F.; Borrie, William T.; O'Loughlin, Jennifer, comps. 2000. Wilderness science in a time of change conference-Volume 5: Wilderness ecosystems, threats, and management; 1999 May 23–27; Missoula, MT. Proceedings RMRS-P-15-VOL-5. Ogden, UT: U.S. Department of Agriculture, Forest Service, Rocky Mountain Research Station. p. 283-287 015.

Schoennagel, T., J. K. Balch, H. Brenkert-Smith, P. E. Dennison, B. J. Harvey, M. A. Krawchuk, N. Mietkiewicz, P. Morgan, M. A. Moritz, R. Rasker, M. G. Turner, and C. Whitlock. 2017. Adapt to more wildfire in western North American forests as climate changes. Proceedings of the National Academy of Sciences 114:4582–4590.

Seielstad, C. 2015. Reconsidering wildland fire use: Perspectives from the Northern Rockies | Rocky Mountain Research Station. Page p 207-212 Proceedings of the large wildland fires conference. Forest Service, Rocky Mountain Research Station, Missoula, MT.

Stevens, J. T., M. M. Kling, D. W. Schwilk, J. M. Varner, and J. M. Kane. 2020. Biogeography of fire regimes in western U.S. conifer forests: A trait-based approach. Global Ecology and Biogeography 29:944–955.

Stevens-Rumann, C., and P. Morgan. 2016. Repeated wildfires alter forest recovery of mixed-conifer ecosystems. Ecological Applications 26:1842–1853.

Stevens-Rumann, C., and P. Morgan. 2016. Repeated wildfires alter forest recovery of mixed-conifer ecosystems. Ecological Applications 26:1842–1853.

Stevens-Rumann, C. S., A. T. Hudak, P. Morgan, A. Arnold, and E. K. Strand. 2020. Fuel Dynamics Following Wildfire in US Northern Rockies Forests. Frontiers in Forests and Global Change 3.

Stevens-Rumann, C. S., K. B. Kemp, P. E. Higuera, B. J. Harvey, M. T. Rother, D. C. Donato, P. Morgan, and T. T. Veblen. 2018. Evidence for declining forest resilience to wildfires under climate change. Ecology Letters 21:243–252.

Taylor, A. H. 2000. Fire regimes and forest changes in mid and upper montane forests of the southern Cascades, Lassen Volcanic National Park, California, U.S.A. Journal of Biogeography 27:87–104.

Taylor, A. H., and C. N. Skinner. 2003. Spatial Patterns and Controls on Historical Fire Regimes and Forest Structure in the Klamath Mountains. Ecological Applications 13:704–719.

Tepley, A. J., E. Thomann, T. T. Veblen, G. L. W. Perry, A. Holz, J. Paritsis, T. Kitzberger, and K. J. Anderson-Teixeira. 2018. Influences of fire–vegetation feedbacks and post-fire

recovery rates on forest landscape vulnerability to altered fire regimes. Journal of Ecology 106:1925–1940.

Van Pelt, R., S. C. Sillett, and N. M. Nadkarni. 2004. CHAPTER 3 - Quantifying and Visualizing Canopy Structure in Tall Forests: Methods and a Case Study. Pages 49–72 *in* M. D. Lowman and H. B. Rinker, editors. Forest Canopies (Second Edition). Academic Press, San Diego.

Ward, A., C. A. Cansler, and A. J. Larson. 2017. Black Carbon on Coarse Woody Debris in Once- and Twice-Burned Mixed-Conifer Forest. Fire Ecology 13:143–147.

Wei, T., and V. Simko. 2021. R package "corrplot": Visualization of a Correlation Matrix.

Welty, J. L. 2018. Western US 30m Heatload Derived Using McCune and Dylan (2002). U.S. Geological Survey.

Zuur, A. F., E. N. Ieno, N. Walker, A. A. Saveliev, and G. M. Smith. 2009. Mixed effects models and extensions in ecology with R. Springer New York, New York, NY.

Appendix A

Cross Walking Datasets

The fire atlas (Green dataset), developed by Patricia Green, retired USFS forest ecologist, was generated from historical drawn fire perimeters for 1870-1880 fires and aerial imagery for fires from 1880-2000 (Morgan et al. 2008a). Fire year and general location of the fire were determined by USFS Region 1 fire history records, then actual fire perimeters were assessed by ocular analysis of aerial photography. The first aerial imagery was taken from 1927-1928 and was used to delineate fire perimeters from 1870-1926. Fires prior to 1880 were determined by hand drawn fire perimeters on map. From 1927-1954, imagery was temporally and spatially coarse, with an area flown approximately once a decade, with lots of imagery taken in 1948 and 1954. There is a gap in imagery from 1954-1980. After 1980, there was annual imagery from 1980-2000, except for 1996. The smallest fire perimeters were 0.53 ha.

Fire severity was determined by Patricia Green as percent mortality of trees using method of Morrison and Swanson (1990), where > 30% mortality was considered low severity, 30-70% was considered moderate severity, and > 70% mortality is considered high severity. Mortality was determined in aerial photography based on number of snags and percent of forest openings. Due to the coarse temporal and spatial resolution of the dataset, the highest confidence is in the high-severity fire. The smallest severity patch was 0.29 ha.

The other dataset is the Parks et al. (2015a) SBW fire atlas from 1972-2015, which has a minimum fire size of 3.5 ha. It is delineated by dNBR, then segmented by hand. I updated this atlas, calculating dNBR for all fires from 2016-2019 in Google Earth Engine, and estimated dNBR for 2020 using Landsat scenes from September 2019, and September 2020. I then compared the perimeters of the Idaho historical fires database (Weber 2020) with the dNBR for 2016-2020 and added any additional fire perimeters not originally in the historical fires database.

Due to the differences in resolution and methods to create the two datasets, certain steps were necessary to make the two datasets comparable and span the full range of years. The first step in this process was determining the severity of the Parks et al. (2015a) dataset. I did this using the composite burn index (CBI), a field-based fire severity metric that incorporates the mortality of trees and other ground based factors (Key and Benson 2006). I calculated CBI from remotely sensed imagery and benchmarking data using the code and methods from Parks et al. (2019). To determine the cutoff of CBI severity for the Parks et al. (2015a) I created a linear regression model of mortality of large trees (a specific category in CBI classification) by CBI using the benchmarking data of (Parks et al. 2019a) (Figure A1). I then used the Morrison and Swanson (1990) cut offs for severity: >30% mortality was considered low severity, 30-70% was considered moderate severity, and >70% mortality is considered high severity to determine corresponding CBI is for each severity class (Table A1).

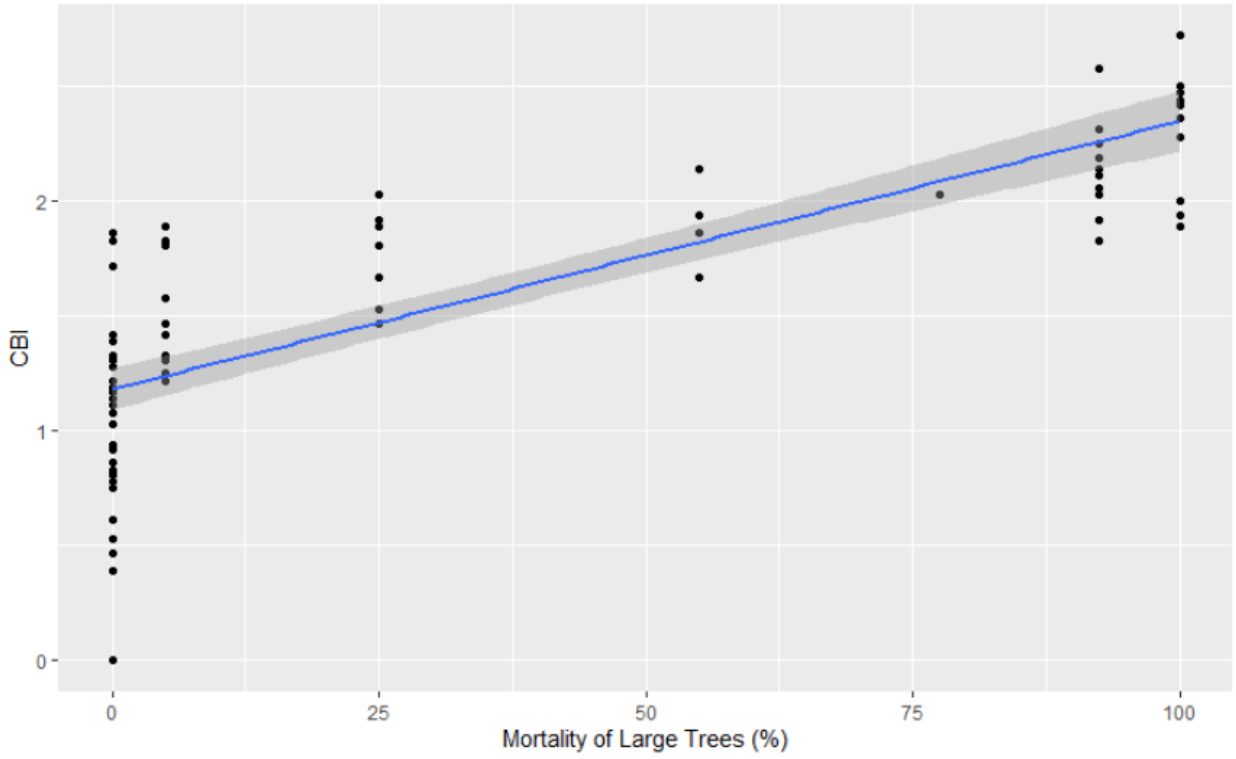

Figure A1. Linear regression of percent mortality by the CBI or large trees.

Table A1. The CBI equivalent of percent mortality for the different severity cutoffs

Severity	% Mortality of Large Trees	CBI
High	<70%	≤2.00
Moderate	20%-70%	1.54-1.99
Low	>30%	≥1.53

I calculated CBI for years 1988-2000 of the Green dataset and subset by the predetermined severities (Figure A2). I calculated CBI for both datasets in these years and there were 641 perimeters in the Green dataset. For all three severity categories, I created histograms

of the distribution of CBI (Figure A2). Seventy percent of pixels in fire perimeters classified as high severity in the Green dataset had a CBI of ≤2.00. For moderate severity patches, 23% of pixels classified as such had a CBI with 1.54-1.99. Low severity patches had a 77% agreement between CBI and the classification of the Green dataset. This made me confident that the Green dataset and the severity derived from CBI dataset are in high agreement of what constitutes as high severity.

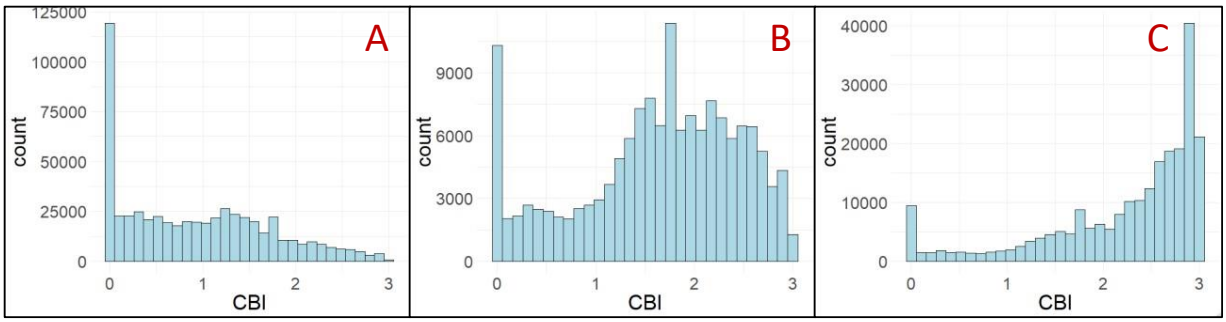

Figure A2. CBI of Green's dataset (A) fire perimeters classified as low severity (B) fire perimeters classified as moderate severity (C) fire perimeters classified as high-severity.

To make the CBI severity classifications within the fire perimeters comparable to the classifications done by photo interpretations in the Green dataset, I took all 1988 fires, a year with both CBI classifications and photo interpretation. I ran the 1988 Green fire perimeters through GEE CBI analysis (Parks et al. 2019a). To make the composition of the CBI classified perimeter smoother and more similar to photointerpretation classification, I ran an averaging moving window summary on CBI within the fire perimeter. Then, I classified pixels with CBI ≥ 2 as high-severity and < 2 as non-high severity. I tried multiple moving windows and used a

confusion matrix to determine which had the highest accuracy. The best window size was 7×7 pixels (210 m × 210 m) (Figure A3) with a confusion matrix accuracy of 74.4% (Table A2).

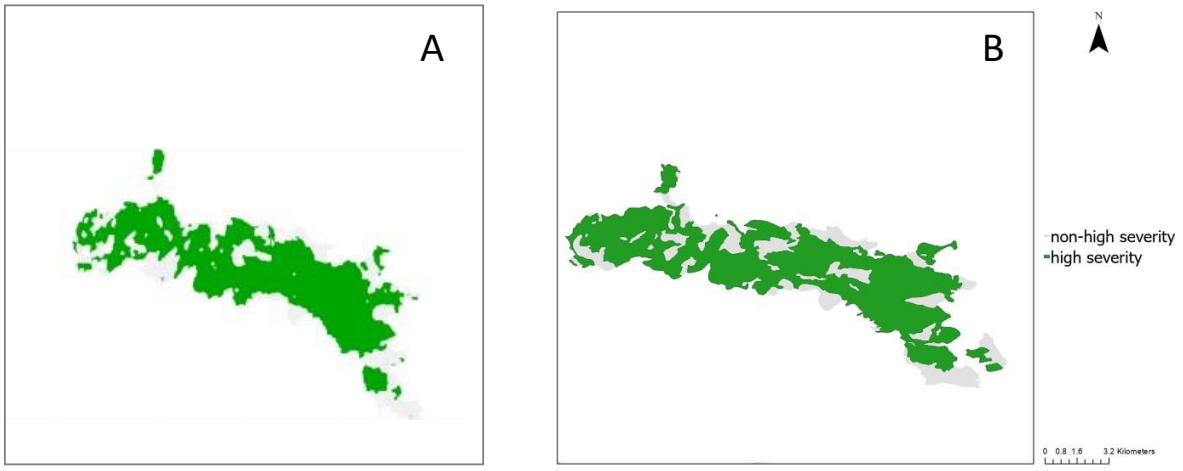

Figure A3. (A) CBI classified fire perimeter with a 7×7 moving window summary. Green is pixels with ≥ 2 CBI and grey < 2 CBI. (B) photo-interpreted classification of severity with green being high-severity and grey non-high severity.

Table A2. Confusion matrix output for 7 × 7 moving window summary.

	Photo-Interpretation Method		
CBI Severity Method		Non-high severity	High-severity
	Non-high Severity	1116490	63203
	High-Severity	33421	164677

To ensure I sampled within high-severity areas and reduce any effect of potential projection or delineation errors and reduce potential edge effects such as the edge of self-limiting fire, I created four-pixel interior buffer (120 m) (Figure A4). This step delineated core high-severity patches.

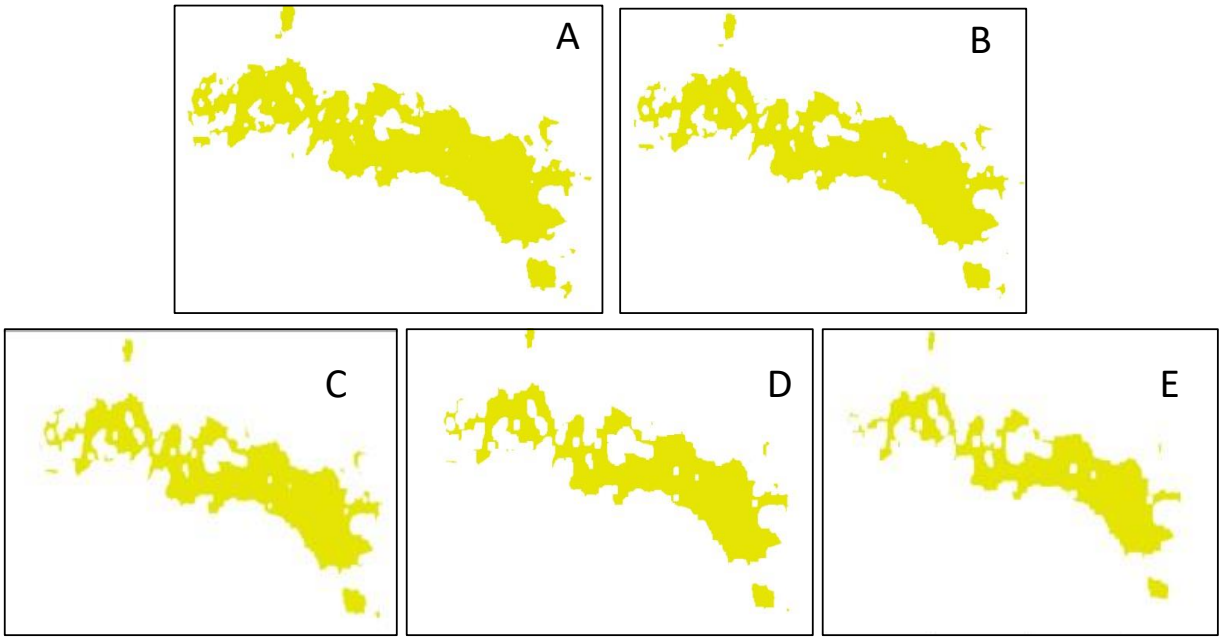

Figure A4. Progression of interior buffering. (A) The initial high-severity patches without buffering for a single example fire perimeter. (B) Buffering by one pixel. (C) Buffering by two pixels. (D) Buffering by three pixels. (E) Buffering by four pixels.

To ensure core high-severity patches of the CBI delineated patches were similar to photo-interpreted high-severity patches on the pixel level I created a confusion matrix comparing core high-severity patches. This analysis showed a 90.1% accuracy (Table A3). Since high-severity patches were of interest, my interior buffering process made all non-core high-severity areas and non-high severity patches valueless (NA) and only input the core-high severity patches into the

confusion matrix. This analysis shows the high level of agreement between the core high-severity patches that are derived from the two methods, which gave me confidence to proceed with field sampling and analysis.

Table A3. Confusion matrix of 7×7pixel moving window summary with 120 m interior buffer.

	Photo-Interpretation Method		
CBI Severity Method		Non-high severity	High-severity
	Non-high Severity	0	0
	High-Severity	10594	96077

I removed all patches that were less than a hectare in size, then I assessed the degree to which patch shapes and sizes were similar between the two methods. I used the landscapemetrics package (Hesselbarth et al. 2019) in R 3.6.1 (R Core Team 2020) that is derived from FRAGSTATS (McGarigal and Marks 1995). This analysis uses a moving window summary for each metric computation and applies an 8-cell neighborhood rule for all raster files. I chose five metrics to describe the patches: mean perimeter area ratio (PARA MEAN), perimeter area ratio standard deviation (PARA SD), mean patch area (AREA MEAN -ha), mean patch perimeter (PERIM MEAN-m), largest patch index (LPI-%). The difference between the CBI method and the photo-interpretation method can be seen in Figure A5. For all fires in 1988, the photo-interpretation method created 49 core high-severity patches and 44 core high-severity patches from the CBI method out of 13 original fire perimeters. Figure A5 shows that both datasets are quite similar across all metrics. The most similar metrics are LPI and AREA MEAN meaning that the sizes of the patches are the very similar, meaning, both methods will delineate severity

patches from the same fire perimeters of similar size, and the largest of the patches are extremely close in size. The two methods had differing size of perimeters, the perimeter to area ratio mean. Despite being of similar size, the shape of the high-severity patches is slightly different. The perimeters are slightly larger and thus the perimeter to area ratio is slightly larger for the Green dataset. Furthermore, the largest difference is the standard deviation between for the Green dataset is much higher than the dataset derived from CBI. This makes a lot of sense that the severity patches created by hand will have more variation and have more irregular shape than computer generated severity patches. Though these differences are small, the difference in LPI is 1.7% and the difference in PARA SD is 29.

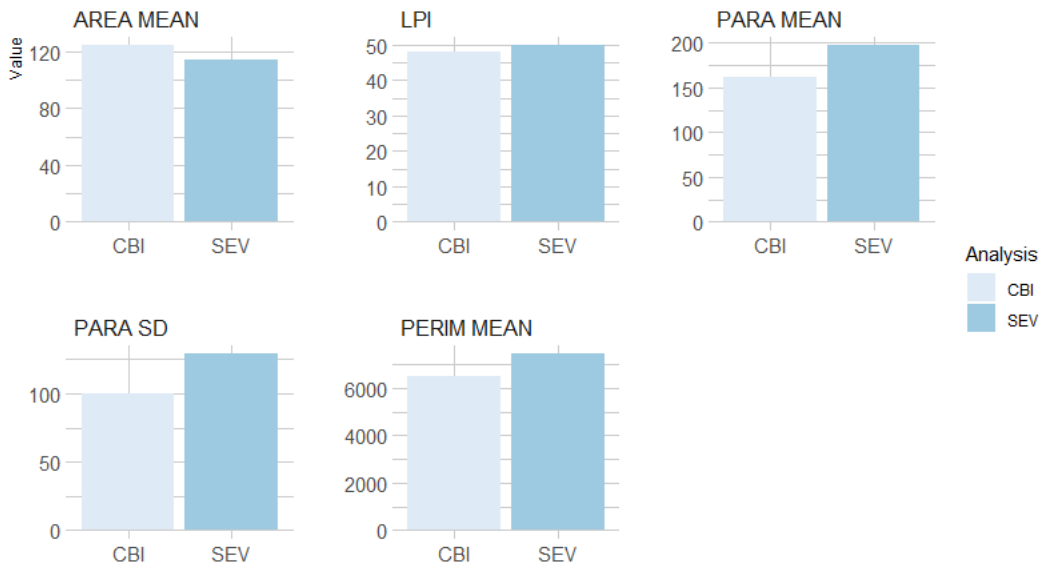

Figure A5. Patch metrics for CBI and photo-interpretation method for core high-severity patches. Variables investigated were mean perimeter area ratio (PARA MEAN), perimeter area ratio standard deviation (PARA SD), mean patch area (AREA MEAN -ha), mean patch perimeter (PERIM MEAN-m), largest patch index (LPI-%).

Literature Cited

Hesselbarth, M. H. K., M. Sciaini, K. A. With, K. Wiegand, and J. Nowosad. 2019. landscapemetrics: an open-source R tool to calculate landscape metrics. Ecography 42:1648–1657.

Key, C. H., and N. C. Benson. 2006. Landscape Assessment (LA):55.

McGarigal, K., and B. J. Marks. 1995. FRAGSTATS: spatial pattern analysis program for quantifying landscape structure. Gen. Tech. Rep. PNW-GTR-351. Portland, OR: U.S. Department of Agriculture, Forest Service, Pacific Northwest Research Station. 122 p 351.

Morgan, P., E. K. Heyerdahl, and C. E. Gibson. 2008. Multi-season climate synchronized forest fires throughout the 20th century, Northern Rockies, USA. Ecology. 89(3): 717-728.:717–728.

Morrison, P. H., and F. J. Swanson. 1990. Fire history and pattern in a Cascade Range landscape. Gen. Tech. Rep. PNW-GTR-254. Portland, OR: U.S. Department of Agriculture, Forest Service, Pacific Northwest Research Station. 77 p 254.

Parks, S. A., L. M. Holsinger, M. J. Koontz, L. Collins, E. Whitman, M.-A. Parisien, R. A. Loehman, J. L. Barnes, J.-F. Bourdon, J. Boucher, Y. Boucher, A. C. Caprio, A. Collingwood, R. J. Hall, J. Park, L. B. Saperstein, C. Smetanka, R. J. Smith, and N. Soverel. 2019. Giving Ecological Meaning to Satellite-Derived Fire Severity Metrics across North American Forests. Remote Sensing 11:1735.

Parks, S. A., L. M. Holsinger, C. Miller, and C. R. Nelson. 2015. Fire atlas for the Selway-Bitterroot Wilderness. Forest Service Research Data Archive.

Appendix B.

Table B1. Species composition faceted by burn history.

Species	Abundance (%)	Burn Abundance
Abies grandis	46%	39%
		34%
		26%
Picea engelmannii	2%	72%
		17%
		10%
Pinus contorta	<1%	0%
		0%
		100%
Pinus ponderosa	8%	25%
		30%
		45%
Pseudotsuga menziesii	33%	34%
		39%
		27%
Thuja plicata	10%	46%
		33%
		21%

Table B2. Fuel loads for fine fuel and litter and duff across all plots mean, median, and standard deviation.

Variable	Fire Frequency	Mean	Median	Standard deviation
1-hr fuels (kg/m^2)	1	0.09	0.06	0.10
	2	0.08	0.05	0.07
	3	0.09	0.05	0.09
10-hr fuels (kg/m^2)	1	0.11	0.04	0.10
	2	0.08	0.05	0.07
	3	0.09	0.06	0.09
100-hr fuels (kg/m^2)	1	0.12	0.05	0.24
	2	0.18	0.08	0.33
	3	0.14	0.05	0.22
Litter depth (cm)	1	1.93	1.75	1.13
	2	1.02	0.98	0.49
	3	0.86	0.69	0.94
Duff depth (cm)	1	1.37	1.25	1.21
	2	0.91	0	2.61
	3	0.54	0.13	0.78

Table B3. Model outputs from linear mixed models of live tree basal area (BA), snag BA, course woody debris (CWD), shrub load, and herb load.

Model	Variable	Estimate	Standard Error	p-value
√(Live tree BA (m^2/ha))	Burned twice	-1.26	0.823	0.14
	Burned thrice	-2.12	0.823	0.02
	TWI	-0.04	0.18	0.81
	Heat load	-2.95	1.26	0.02
√(CWM (m^3/ha)	Burned twice	4.62	3.03	0.15
	Burned thrice	6.46	3.03	0.04
	TWI	1.74	0.95	0.07
	Heat load	-16.50	6.37	0.01
√(Dead tree BA (m^2/ha))	Burned twice	1.81	0.53	0.004
	Burned thrice	1.76	0.52	0.004
	TWI	0.41	0.15	0.01
	Heat load	-1.89	1.05	0.08
√(Shrub load (kg/m^2))	Burned twice	-0.09	0.09	0.33
	Burned thrice	-0.20	0.09	0.83
	TWI	0.003	0.04	0.94
	Heat load	0.41	0.25	0.11
√(Herb load (kg/m^2))	Burned twice	-0.002	0.02	0.92
	Burned thrice	-0.01	0.02	0.54
	TWI	0.01	0.01	0.31
	Heat load	0.03	0.06	0.61

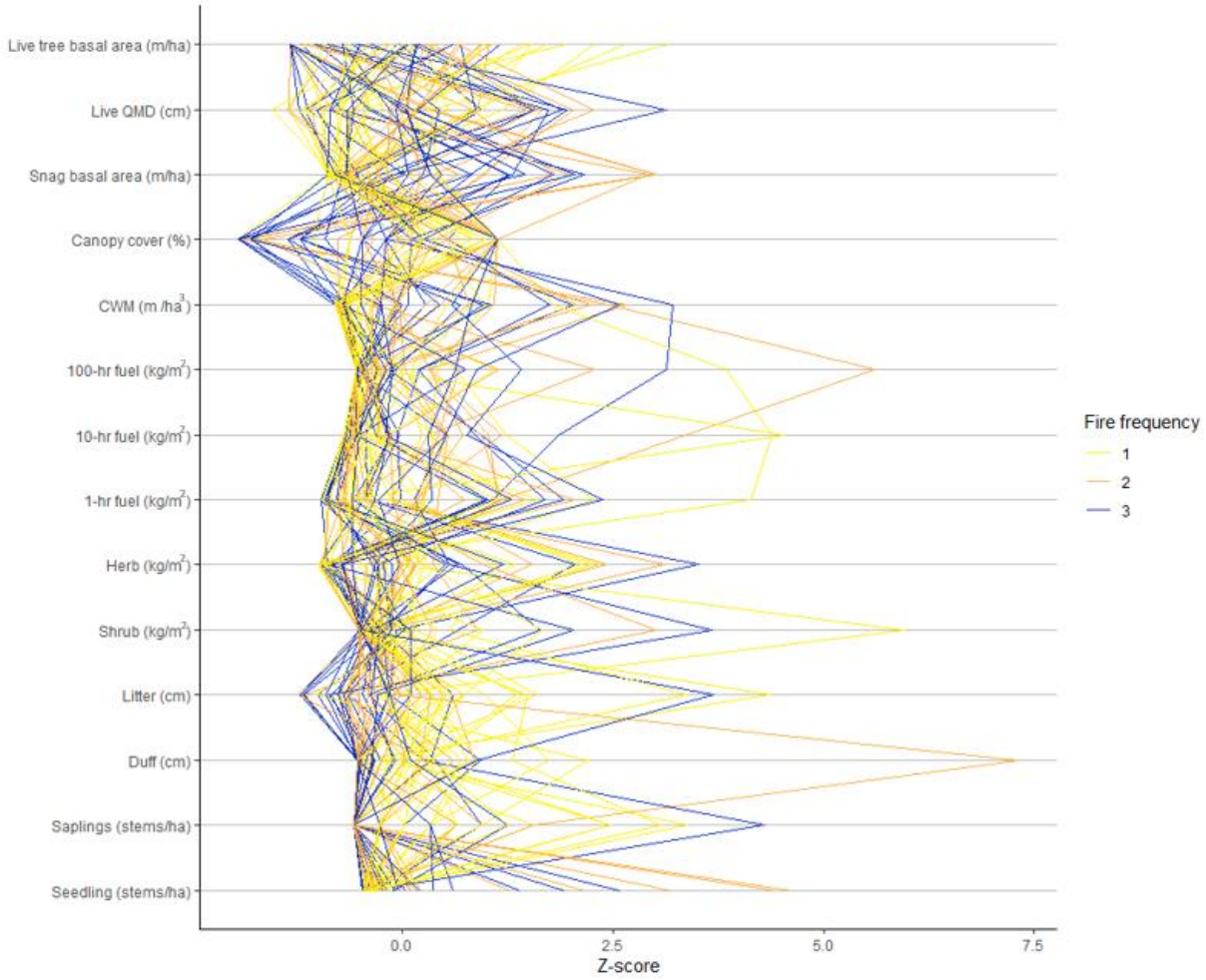

Figure B1. A parallel plot diagram depicting all structural and fuel variables of interest. Each line represents a plot, and they move across the x-axis depending on the Z-score for a particular variable.

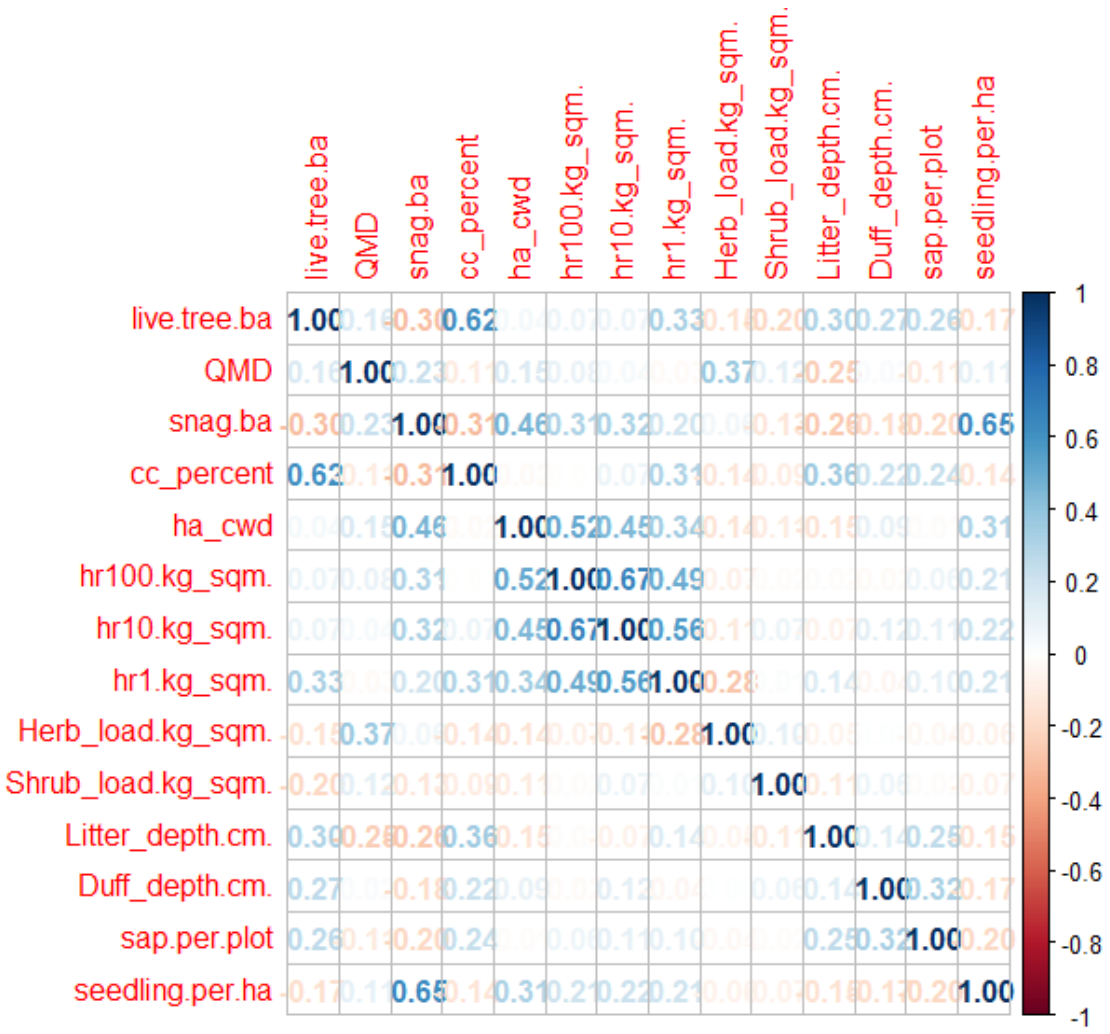

Figure B2. Correlation of variables used in the PCA analysis.